

## A Road Map for the Generation of a Near-Infrared Guide Star Catalog for Thirty Meter Telescope Observations

Smitha Subramanian<sup>1,2,\*</sup>, Annapurni Subramaniam<sup>1</sup>, T. Sivarani<sup>1</sup>, Luc Simard<sup>3</sup>, G. C. Anupama<sup>1</sup>, Kim Gillies<sup>4</sup>, A. N. Ramaprakash<sup>5</sup> & B. Eswar Reddy<sup>1</sup>

<sup>1</sup>*Indian Institute of Astrophysics, Koramangala, Bangalore 560 034, India.*

<sup>2</sup>*Kavli Institute for Astronomy & Astrophysics, Peking University, Beijing 100871, China.*

<sup>3</sup>*National Research Council of Canada, Herzberg Institute of Astrophysics, 5071 West Saanich Road, Victoria, British Columbia, Canada.*

<sup>4</sup>*Thirty Meter Project Office, Pasadena, California, USA.*

<sup>5</sup>*Inter University Center for Astronomy & Astrophysics, Pune 411 007, India.*

\**e-mail: smithahsharma@gmail.com*

Received 20 April 2016; accepted 1 August 2016

**Abstract.** The near-infrared instruments in the upcoming Thirty Meter Telescope (TMT) will be assisted by a multi conjugate Adaptive Optics (AO) system. For the efficient operation of the AO system, during observations, a near-infrared guide star catalog which goes as faint as 22 mag in  $J_{\text{Vega}}$  band is essential and such a catalog does not exist. A methodology, based on stellar atmospheric models, to compute the expected near-infrared magnitudes of stellar sources from their optical magnitudes is developed. The method is applied and validated in JHKs bands for a magnitude range of  $J_{\text{Vega}}$  16–22 mag. The methodology is also applied and validated using the reference catalog of PAN STARRS. We verified that the properties of the final PAN STARRS optical catalog will satisfy the requirements of TMT IRGSC and will be one of the potential sources for the generation of the final catalog. In a broader context, this methodology is applicable for the generation of a guide star catalog for any existing/upcoming near-infrared telescopes.

*Key words.* Stars—near-infrared magnitudes—adaptive optics.

### 1. Introduction

Thirty Meter Telescope (TMT) is an advanced, wide field (20 arcmin), altitude-azimuth telescope with a primary mirror consisting of 492 segments. The telescope is planned for installation on the summit of Mauna Kea on the island of Hawaii in

the United States. The near-infrared instruments of TMT will be assisted by a multi conjugate adaptive optics system, Narrow Field Infrared Adaptive Optics System (NFIRAOS), and for the efficient operation of this system, a near-infrared guide star catalog is essential. The TMT Infra Red Guide Star Catalog (TMT-IRGSC) will be a star catalog consisting of point sources with JHKs magnitudes in Vega system, with  $J_{\text{Vega}}$  magnitudes as faint as 22, covering the entire TMT-observable sky from  $+90^\circ$  to  $-45^\circ$  declination. The TMT-IRGSC will be a critical resource for TMT operations that enables efficient planning and observing fulfilling a role similar to that of the Guide Star Catalog I and II, which were created to enable acquisition and control of the Hubble Space Telescope. No catalog currently exists with objects this faint in the IR over a large enough area of the sky to be useful as a guide star catalog. It is highly essential to develop this catalog by computing the expected NIR magnitudes of stellar sources using their observed optical magnitudes.

In a feasibility study, Subramanin *et al.* (2013) (hereafter S12) identified the requirements of the TMT IRGSC and presented a methodology based on black body model for the computation of the expected  $J_{\text{Vega}}$  magnitude of stellar sources from their optical magnitudes ( $g$ ,  $r$  and  $i$  band magnitudes). They applied and verified the methodology in three test fields identified from the Canada France Hawaii Telescope (CFHT) legacy survey with  $g$ ,  $r$ ,  $i$  band observations and complementary NIR observations from UKIRT surveys. The methodology developed was applied to the probable stellar sources (which were classified based on their extent on the sky) and the computed  $J_{\text{Vega}}$  magnitudes were compared with the observed  $J_{\text{Vega}}$  magnitudes. This was found to be satisfactory for the magnitude range,  $J_{\text{Vega}} = 16\text{--}20$  mag in the three test fields. The brighter sources were saturated in the optical bands and for the fainter sources the star/galaxy classification was not available.

The important requirements of the TMT IRGSC identified by S12, which play major role in the development of the methodology for the computation of NIR magnitudes are

- (a) *Limiting magnitude*: There should be sources as faint as  $J_{\text{Vega}} = 22$  mag,
- (b) *Errors*: The NIR magnitudes should have an error  $\leq 0.2$  mag
- (c) *Source density criteria of NFIRAOS*: Availability of at least 3 stars in 2 arcmin diameter field-of-view which corresponds to nearly 3440 stars in one square degree field.

To validate the methodology for fainter magnitudes, we have to develop an optimal method for the star/galaxy separation of the fainter optical sources. Also the computation of H and Ks band magnitudes is essential for the generation of the catalog. The stars are not perfect black bodies and we have to incorporate more realistic stellar models to compute the infrared magnitudes from their optical magnitudes.

The scope of the present work is to improve the methodology developed by S12 by incorporating more realistic stellar models for the computation of the NIR magnitudes and to satisfy the requirements of the TMT IRGSC. Moreover, we assess the predicted properties of the final PAN-STARRS optical catalog and check whether they satisfy the requirements of the TMT IRGSC, hence creating a road map for the final production of the TMT IRGSC.

## 2. Extension of star/galaxy classification

The test fields used by S12 for the application and validation of their methodology were from the CFHT Legacy Survey (CFHTLS) wide/deep fields (with optical data in  $g, r, i$  bands) which have NIR data from UKIRT Large Area Survey (LAS) or UKIRT Deep Extragalactic Survey. The details of the test fields are given in Table 1. The reddening values adopted for these fields from Schlegel *et al.* (1998) are also given in the table. The star/galaxy classification of the sources in the optical catalog of those fields was based on their spatial extent on the sky. The probable stellar sources follow a horizontal locus in the half-light radius vs.  $I_{AB}$  plot as shown in Fig. 1. The criteria used for the identification of stellar sources were half-light radius  $< 0.5$  arcsec and  $I_{AB} = 17-21$  mag. The computed  $J_{Vega}$  magnitude of the sources identified by these criteria did not go as faint as 22 mag in  $J_{Vega}$ , which is one of the requirements of TMT IRGSC. Thus it is essential to extend the star/galaxy classification to the fainter end of optical magnitudes.

**Table 1.** Details of the test fields. Each test field covers  $1 \text{ deg}^2$  in the sky.

No.	Centre coordinates	Optical data (CFHTLS)	NIR data (UKIDSS)	$E(B-V)$
T1	RA = $150^{\circ}.10$ , Dec. = $2^{\circ}.20$ $l = 237^{\circ}.52$ , $b = 42^{\circ}.83$	Deep field ( $gri$ )	LAS (JHKs) with J up to 20 mag	0.02 mag
T2	RA = $334^{\circ}.27$ , Dec. = $0^{\circ}.38$ $l = 63^{\circ}.08$ , $b = -43^{\circ}.84$	Wide field ( $gri$ )	DXS(JKs) with J up to 22 mag	0.06 mag
T3	RA = $332^{\circ}.37$ , Dec. = $0^{\circ}.52$ $l = 61^{\circ}.59$ , $b = -42^{\circ}.28$	Wide field ( $gri$ )	LAS (JHKs), with J up to 20 mag	0.04 mag

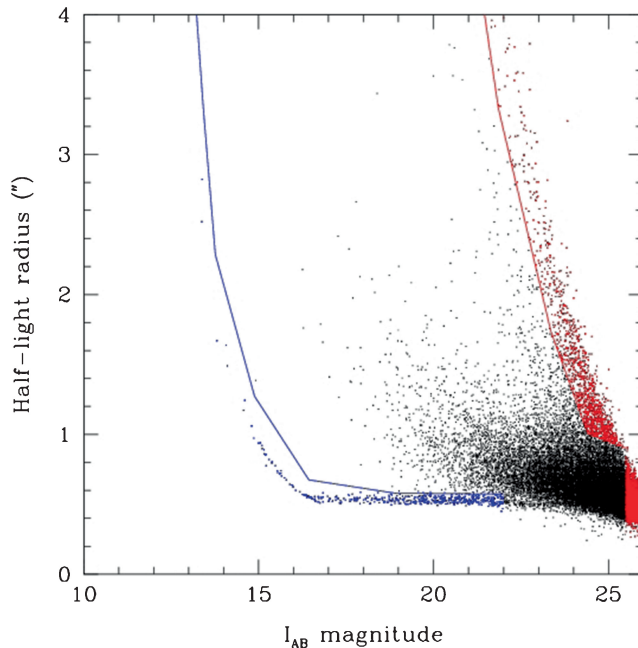


**Figure 1.**  $I_{AB}$  magnitude vs. half-light radius plot of all the sources in the CFHTLS field. The blue points are the stellar sources, red points are spurious objects and the black points are the galaxies. The blue line is the locus of the stars.

As an initial step, colour–colour diagrams (CCD) are analysed as a tool for star/galaxy classification. Based on the location of the sources in the CCD we can classify them. The sources from the test field, T2 (1 deg<sup>2</sup> sub-region of CFHTLS wide field W4) of S12 are analysed. In Fig. 2 the sources which are classified as probable stellar sources (half-light radius < 0.5 arcsec and  $I_{AB} = 17\text{--}21$  mag) and galaxies, based on the CFHTLS flagging criteria, are shown in the  $(g-r)$  vs.  $(r-i)$  CCD. The upper panel shows the galaxies and lower panel shows the stars. From the figure we can see that the stars occupy a tight locus in the CCD, whereas galaxies are scattered. Though there is an overlap in the location of stars and galaxies, the tight locus of stars can be used as a classification tool.

Now to extend the star/galaxy classification beyond  $I_{AB} = 21$  mag, we selected sources within the magnitude range of 21–24 in  $I_{AB}$  and with half-light radius value less than 0.5 arcsec. The CCD of these sources is analysed. The lower, middle and upper panels of Fig. 3 show the CCD of sources in the magnitude range 21–22, 22–23 and 23–24 (shown as black points) over plotted on the CCD of probable stellar sources (with  $17 \leq I_{AB} \leq 21$ ) which are shown as red points. The lower and middle panels suggest that the locus of black points in these panels are similar to that of the

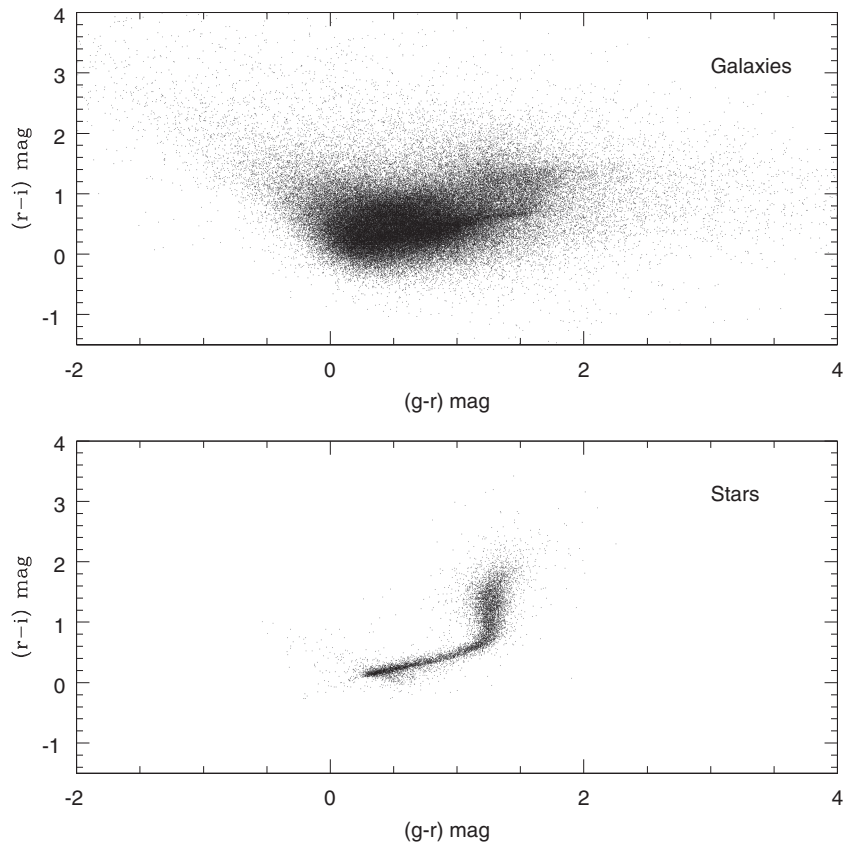


**Figure 2.** The  $(g-r)$  vs.  $(r-i)$  colour–colour diagram of probable stellar sources (half-light radius < 0.5 arcsec and  $I_{AB} = 17\text{--}21$  mag) and galaxies which are classified based on their spatial extent for the test field, T2 of S12.

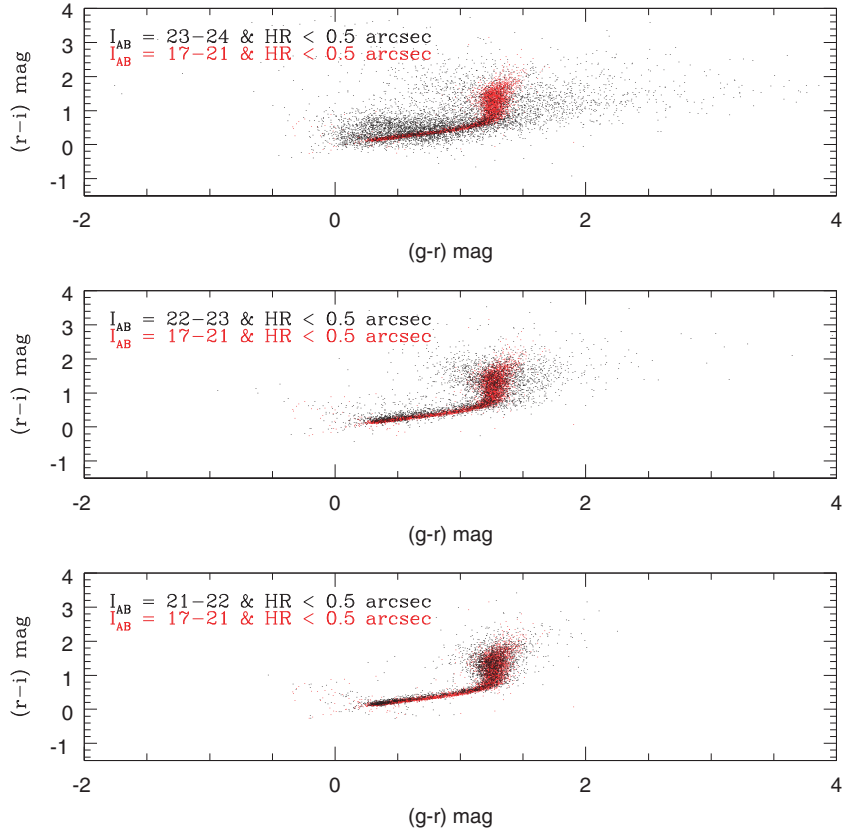


**Figure 3.** The CCD of sources, shown as black points, with  $I_{AB}$  beyond 21 mag over plotted on the CCD of probable stellar sources ( $I_{AB} = 17-21$  mag and half-light radius  $< 0.5$  arcsec which are shown as red points). The black points in the lower, middle and upper panels show the sources in the magnitude range  $I_{AB} = 21-22$  mag,  $I_{AB} = 22-23$  mag and  $I_{AB} = 23-24$  mag respectively.

probable stellar sources. They are tightly distributed. On the other hand, the black points in the upper panel are scattered and do not follow any pattern. This suggests that the star/galaxy classification based on half-light radius can be extended up to  $I_{AB} = 23$  mag. Sources with  $I_{AB}$  up to 23 mag may be sufficient to produce a catalog with sources up to  $J_{Vega} = 22$  mag. Again, including fainter sources will help to increase the source density and hence satisfy the source density criteria of NFIRAOS.

### 3. Application of S12 model

In order to check whether the extension of the star/galaxy classification is enough to satisfy the magnitude requirement of the TMT IRGSC, we applied the methodology developed by S12 to the stellar sources, identified using the extended classification criteria (sources with  $17 < I_{AB} < 23$  mag, and half-light radius less than  $\sim 0.5$  arcsec), in the test field T2 (1 deg<sup>2</sup> sub-region of CFHTLS wide field W4 which has optical data in  $g, r, i$  bands from CFHTLS and NIR data from deep extragalactic survey

of UKIDSS, refer Table 1 for more details of the test fields). We cannot extend the classification criteria in the brighter end,  $I_{AB} < 17$  mag, because the sources are saturated. The probable stellar sources with NIR counterparts in the test field T2 after applying the new classification criteria are 3695. For these sources the  $J_{Vega}$  mag and the associated error are calculated (using the methodology provided by S12). The errors are estimated by propagating the errors in the observed optical magnitudes in each step of the computation of the NIR magnitudes. The computed magnitudes are compared with the observed magnitudes. Figure 4 shows the difference in the observed and computed magnitudes of these sources plotted against the observed magnitudes. The different panels represent the computed magnitudes based on the scaling factors estimated in different bands. The scaling factor is defined as the ratio of observed flux to the absolute flux from the model in each optical band, which is used for the computation of the expected NIR fluxes (see S12 for more details). The

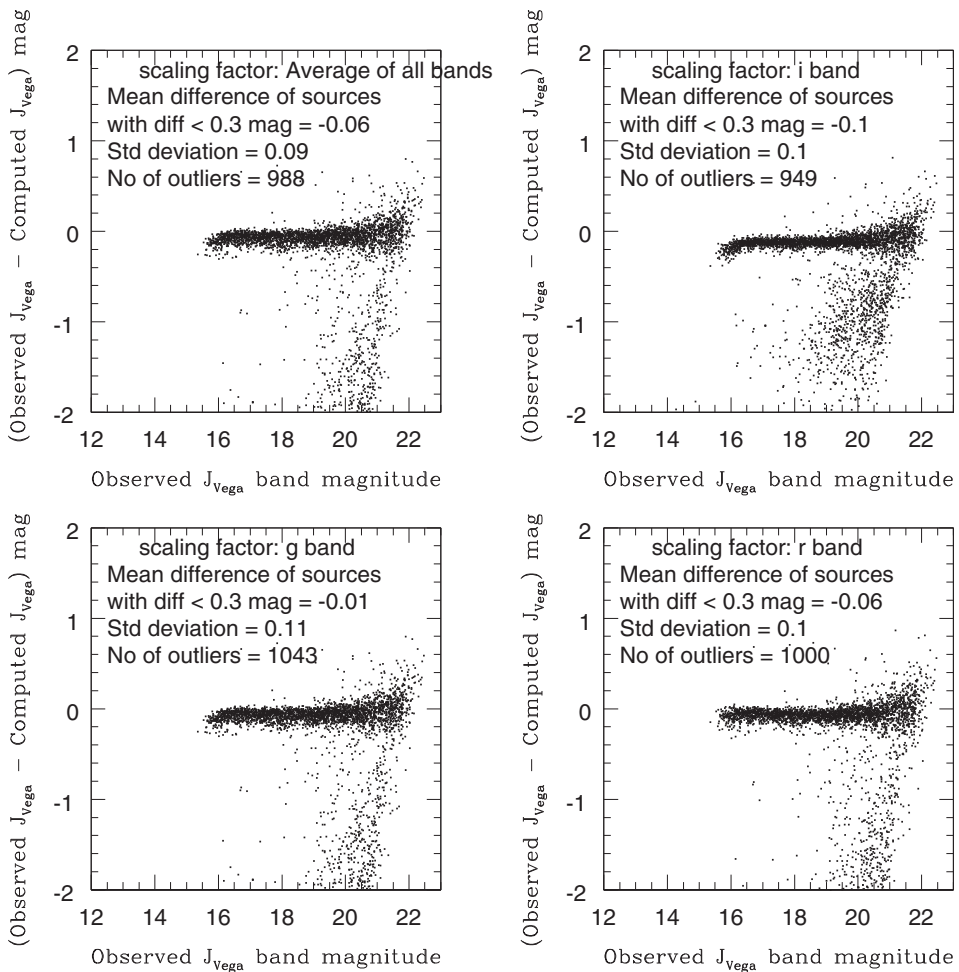


**Figure 4.** For the 3695 probable stellar sources (identified using the extended star/galaxy criteria) in the test field, T2, the difference between the observed and computed magnitudes are plotted against the observed  $J_{Vega}$  magnitude.

scaling factors are calculated using the observed and computed optical magnitudes of the sources in the optical catalog. Then they are applied to the absolute NIR magnitudes to calculate the expected apparent NIR magnitudes. The mean difference between the observed and computed magnitudes and the scatter are very similar in all the four panels. This suggests that the effect of different scaling factors (obtained from different optical bands) is very minimal in the computation of the NIR magnitudes. The computed magnitudes of  $\sim 60\%$  sources in the fainter end ( $J_{\text{Vega}} = 20\text{--}22$  mag) matches with the observed magnitudes within 0.3 mag (the error associated with the difference between the computed and the observed magnitudes is  $\sim 0.1$  mag and  $0.3$  mag = 3 times the error). This suggests that the methodology developed by S12 is applicable for the computation of magnitudes up to  $J_{\text{Vega}} = 22$  mag. From this analysis, we also found that for the production of final TMT IRGSC (with a limiting magnitude of  $J_{\text{Vega}} = 22$  mag), we need sources with  $g, r, i$  bands optical data which goes as deep as  $I_{\text{AB}} = 23$  mag. This could be tested only in T2 as we do not have NIR observations beyond  $J_{\text{Vega}} = 20$  mag in the other test fields of S12, to compare with the computed magnitudes. But, when fainter sources are included by extending the star/galaxy classification, the number of outliers increases. This can be due to the contamination of non-stellar sources and/or due to limitation of the black body model used by S12. With photometric information in three bands we cannot improve the star/galaxy classification further at this point.

Another requirement of TMT IRGSC is that the stellar sources should have magnitudes in JHKs bands in Vega system. More specifically the  $(J - Ks)_{\text{Vega}}$  and  $(H - Ks)_{\text{Vega}}$  colours are required along with the  $J_{\text{Vega}}$  magnitudes in the TMT IRGSC. S12 only computed the  $J_{\text{Vega}}$  magnitudes and compared with the observed values. The  $H_{\text{Vega}}$  and  $Ks_{\text{Vega}}$  magnitudes are computed by integrating the black body function, corresponding to the temperature of the sources, using the H and Ks pass bands (similar to the method described in S12 for the computation of  $J_{\text{Vega}}$ ). The sources in the test fields have UKIRT NIR data for comparison with the computed magnitudes and hence the UKIRT WFCam response functions are used during the computation of the magnitudes. We computed the H and Ks magnitudes in Vega system of probable stellar sources in the three test fields, T1, T2 and T3 of S12 (all these test fields are  $1 \text{ deg}^2$  sub-region from the CFHTLS fields with NIR observations in UKIRT surveys, refer Table 1 for the details of these test fields). The test fields T1 and T3 have NIR observations only up to  $J_{\text{Vega}} = 20$  mag and hence the comparison of the computed and observed magnitudes for the sources in T1 and T3 are restricted only up to  $J_{\text{Vega}} = 20$  mag. Hence for these fields (hereafter this is applicable for the fields T1 and T3 in all the sections of the paper) we do not apply the extended star/galaxy classification as we cannot validate it by comparing the computed and the observed NIR magnitudes. The difference between the observed and computed  $H_{\text{Vega}}$  magnitudes of the probable stellar sources in the test fields, T1 and T3 are plotted against their observed  $H_{\text{Vega}}$  magnitudes in Figures 5 and 6. For the test field, T2 observed H band data are not available. So the calculated H band magnitudes of the probable stellar sources in this field are not compared with the observed magnitude. The difference between the observed and computed  $Ks_{\text{Vega}}$  magnitudes of the probable stellar sources in the test fields, T1, T2 and T3 are plotted against their observed  $Ks_{\text{Vega}}$  magnitude in Figures 7, 8 and 9 respectively. The average error associated with the difference between the computed and observed  $H_{\text{Vega}}$  and  $Ks_{\text{Vega}}$  magnitudes are  $\sim 0.1$  mag. Hence the sources which show a difference between the observed and computed magnitudes greater than 0.3 mag are considered as outliers.

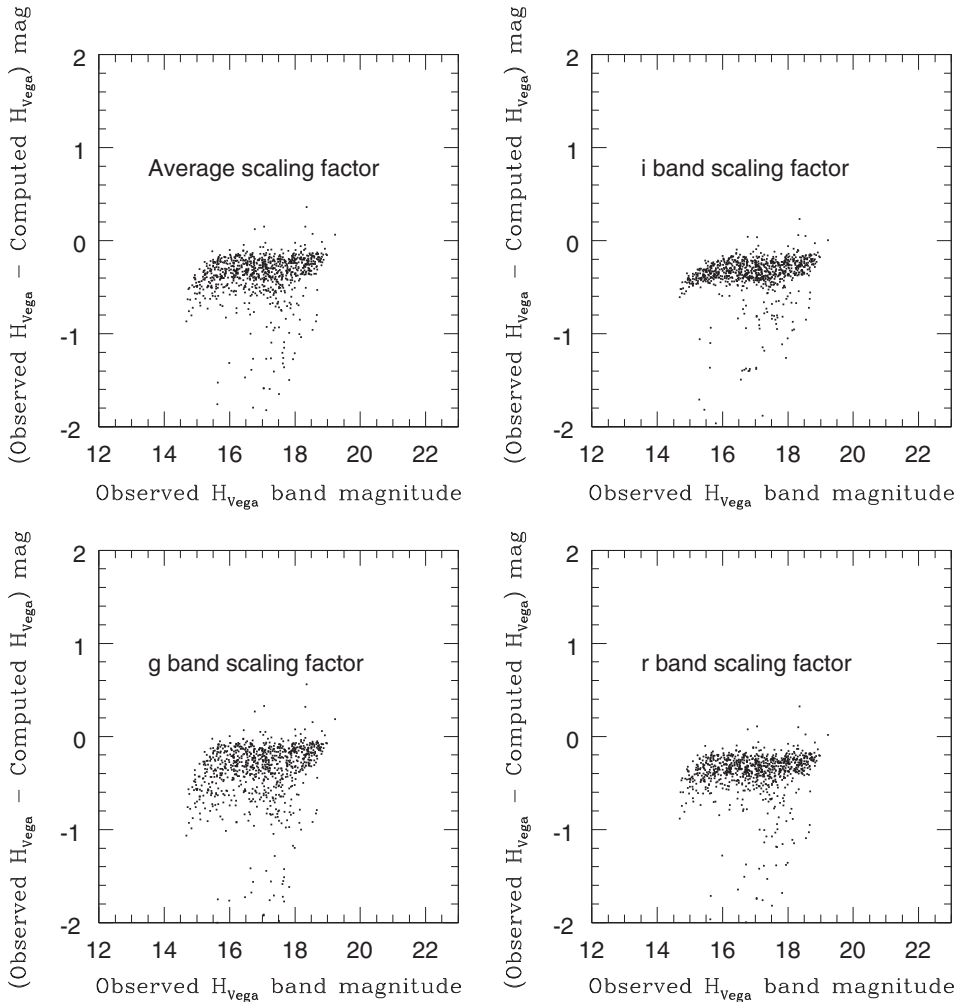


**Figure 5.** For the 868 probable stellar sources in the test field, T1, the difference between the observed and computed H band magnitudes are plotted against the observed  $H_{\text{Vega}}$  magnitude.

The results of our analysis, based on the black body model, on different test fields are summarised in Table 2. From Table 2 and the comparison plots we can see that the methodology developed by S12 is applicable for the computation of  $H_{\text{Vega}}$  and  $Ks_{\text{Vega}}$  magnitudes as well. The mean difference between the observed and computed magnitudes while comparing the computed  $H_{\text{Vega}}$  and  $Ks_{\text{Vega}}$  magnitudes with the observed are shifted to the negative values. This means that the computed magnitudes are fainter than the observed magnitudes. A similar, but less significant trend is seen in the case of  $J_{\text{Vega}}$  computation also (Fig. 4). One of the probable reasons for this shift can be the limitation of the black body model. In reality, the stars do not act as perfect black bodies. The atmosphere of stars absorbs light and it reduces the flux. Thus the flux computed in each band, based on black body model will be higher than the actual flux we receive from the star. The absorption features are more in the optical bands when compared to infrared bands. We use the computed optical fluxes

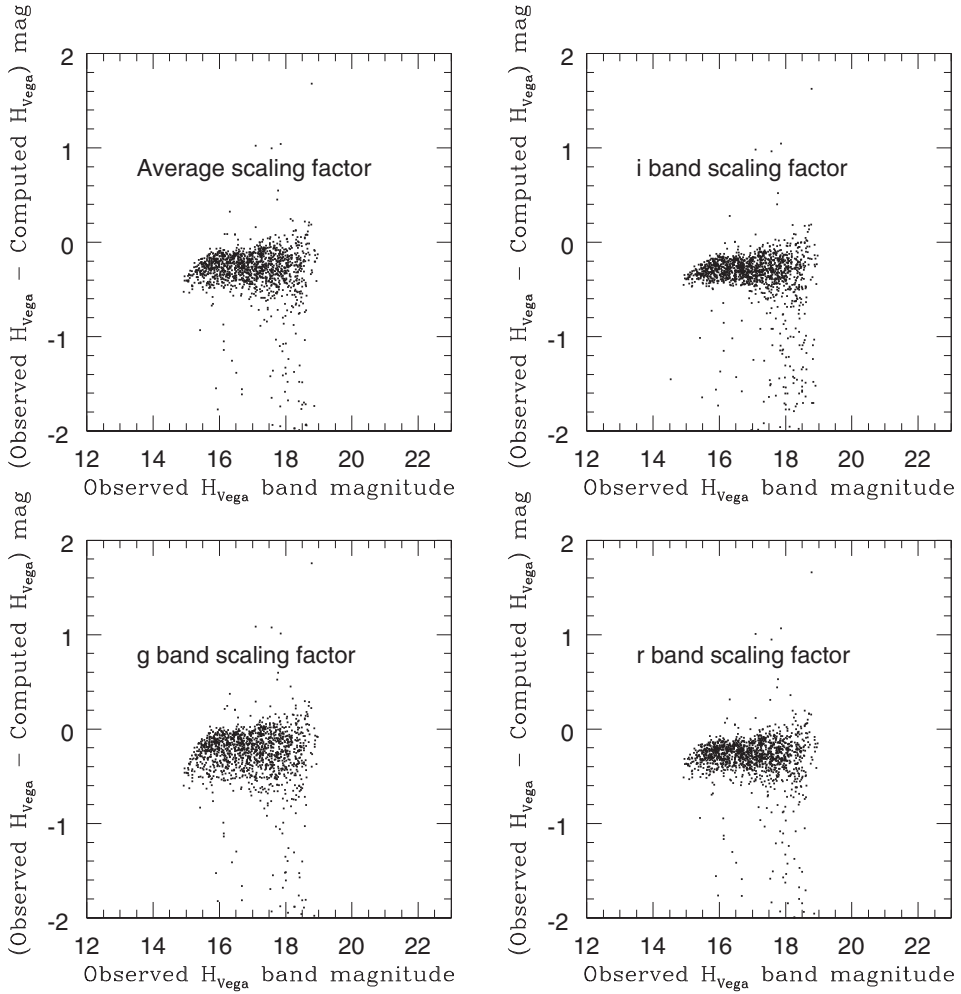


**Figure 6.** For the 2013 probable stellar sources in the test field, T3, the difference between the observed and computed magnitudes are plotted against the observed  $H_{\text{Vega}}$  magnitude.

to estimate the scaling factor, by comparing the computed magnitude with the observed magnitude. Thus the estimated scaling factor will be more than the actual one. This scaling factor is used to convert the computed absolute JHKs band flux to the apparent  $J_{\text{Vega}}$ ,  $H_{\text{Vega}}$  and  $K_{\text{Svega}}$  band fluxes. As the scaling factor is higher than the actual value, the computed flux will be less and hence the magnitudes will be fainter. As the absorption in infrared bands is much lower, the computed absolute flux is comparable with the actual one and so will not have significant effect on the computed magnitude. Thus the limitation in the model we use makes the computed magnitudes fainter. Hence the difference becomes negative. We can rectify this by using stellar atmospheric models for the computation of magnitudes. Other possibilities for the discrepancies are the uncertainty in the temperature estimates and reddening values. The computed magnitudes can be fainter than the observed one if the reddening values and temperatures are underestimated.

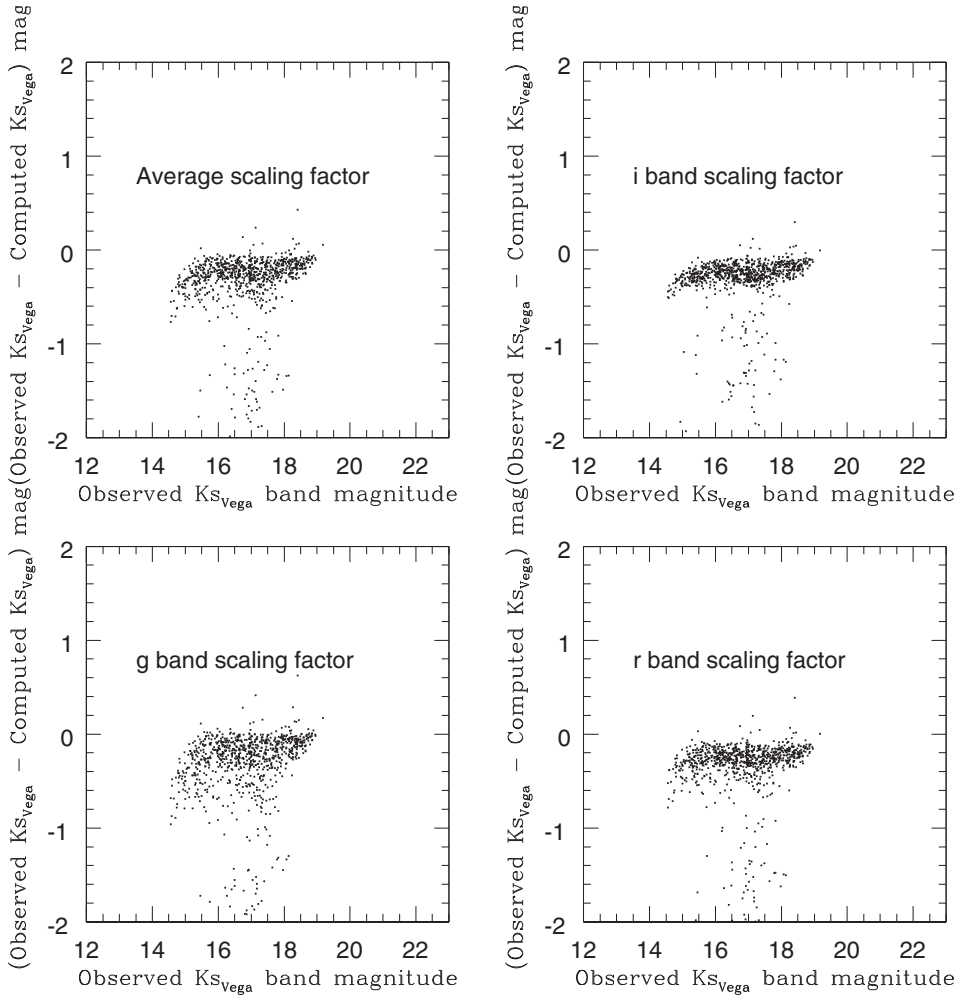


**Figure 7.** For the 868 probable stellar sources in the test field, T1, the difference between the observed and computed Ks band magnitudes are plotted against the observed  $Ks_{Vega}$  magnitude.

To improve the methodology developed by S12, we need to incorporate more realistic stellar atmospheric models. Along with the improvement in the computed NIR magnitudes, the stellar atmospheric models themselves may remove non stellar sources from the optical catalog. The observed number of outliers in the fainter end of all the comparison figures may reduce if we use the methodology based on stellar atmospheric models.

#### 4. Stellar models

To include the effect of stellar absorption in the computed magnitudes, we incorporated stellar atmospheric models in the methodology. We used the PHOENIX/NextGen model (Hauschildt *et al.* 1999a, b) and Kurucz/ATLAS model

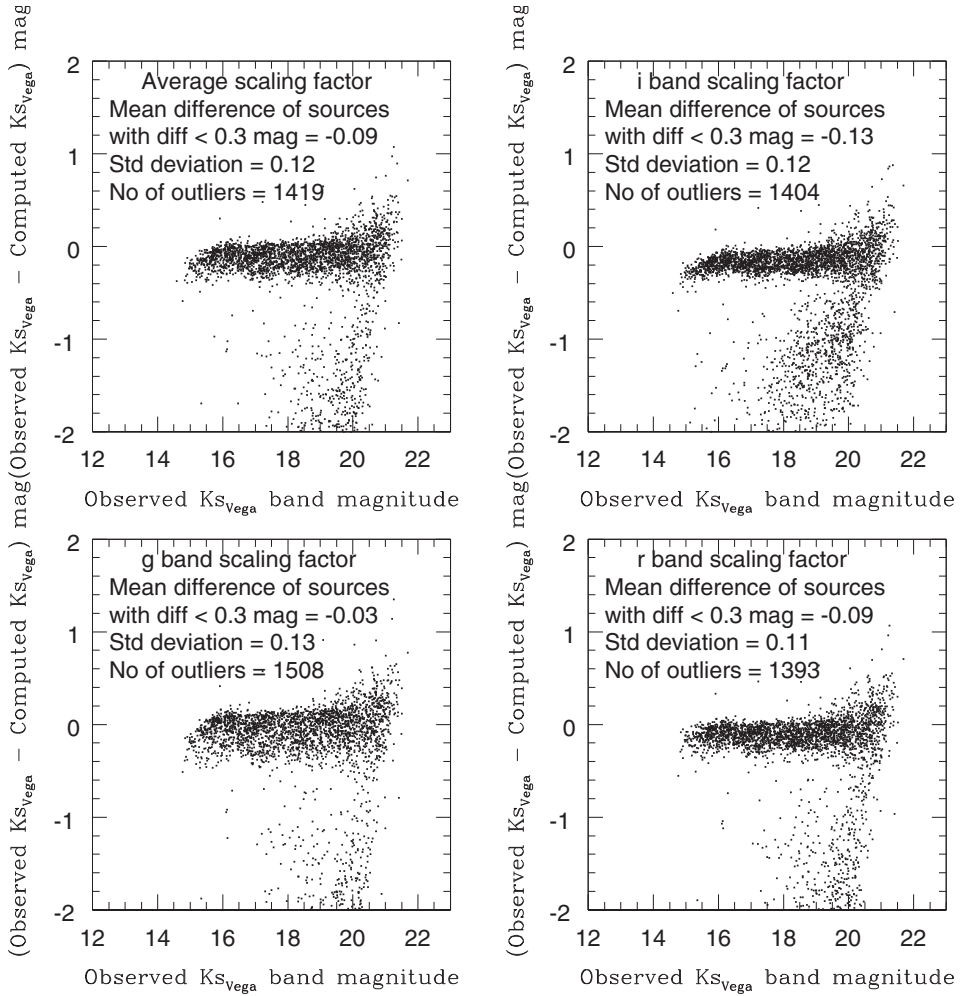


**Figure 8.** For the 3695 probable stellar sources (identified using the extended star/galaxy criteria) in the test field, T2, the difference between the observed and computed magnitudes are plotted against the observed  $K_{s,Vega}$  magnitude.

(Kurucz 1992a, b, 1993, 1995; Castelli *et al.* 1997) to compute the expected JHKs magnitudes of probable stellar sources in the test fields. The grid parameters and their range of these two models are given as

*Kurucz–Castelli model:* Grid coverage:  $3500 < T_{\text{eff}} < 500000$  K;  $+3.5 < \log(g) < 6.0$ ;  $4.0 < [\text{Fe}/\text{H}] < +0.0$ ;  $10 \text{ nm} < \lambda < 1000000$  nm.

*Next-gen model:* Grid coverage:  $1000 \text{ K} < T_{\text{eff}} < 10000$  K;  $+0.0 < \log(g) < +5.0$ ;  $-5.0 < [\text{Fe}/\text{H}] < +1.0$ ;  $9.1 \text{ nm} < \lambda < 160000$ .

The temperature grid spacing in Kurucz model is 250 K for the whole temperature range. In NextGen model the temperature grid spacing is 100 K in the temperature range 2700–7000 K and it is 200 K in the temperature range 7000–10000 K.

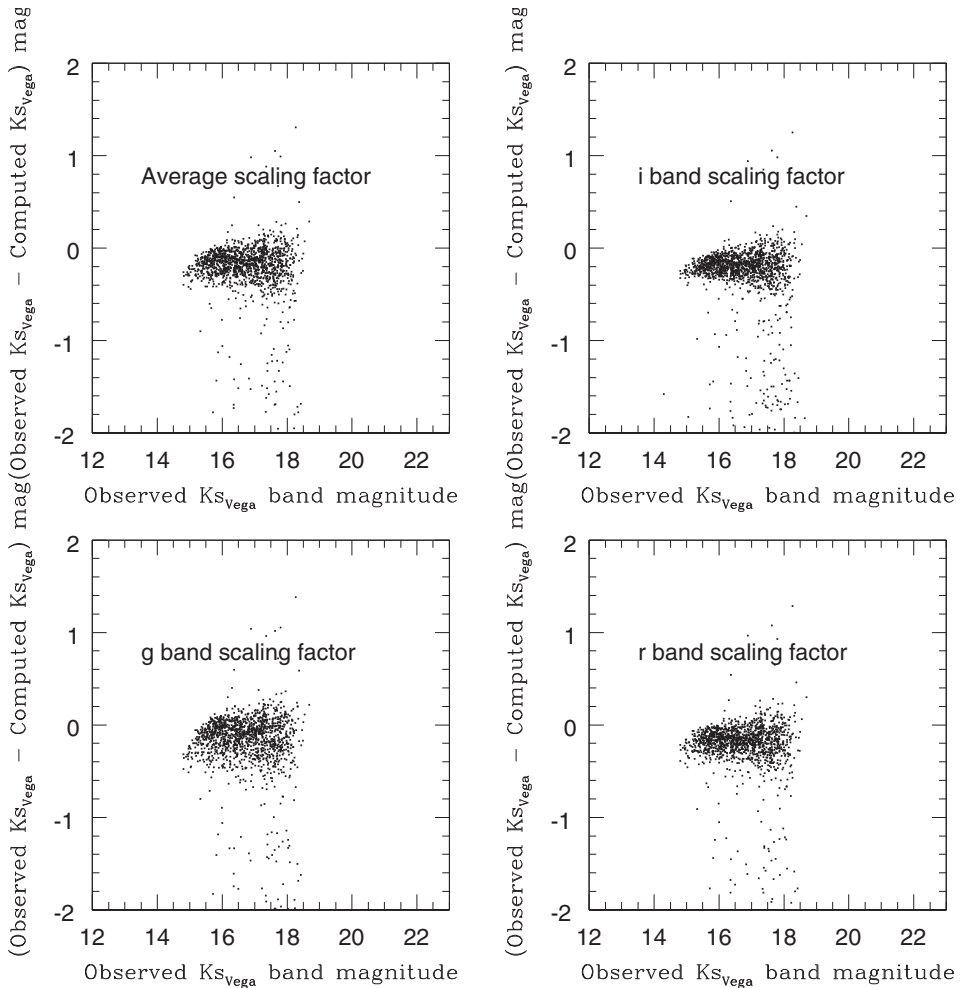


**Figure 9.** For the 2013 probable stellar sources in the test field, T3 the difference between the observed and computed magnitudes are plotted against the observed  $Ks_{Vega}$  magnitude.

#### 4.1 Methodology based on stellar atmospheric models

The stellar models generate synthetic colours and magnitudes of stars at the stellar surface with different stellar atmospheric parameters like effective temperature, gravity and metallicity. These parameters define the model of each star. The synthetic colours and magnitudes in the 2MASS and SDSS filters are obtained. The synthetic colours and magnitudes in the filter system we require can be obtained by incorporating the corresponding filter response functions. As the template in the SDSS and 2MASS filters were readily available, we used them and converted the colours and magnitudes to our required filter systems using the transformation equations (Gwyn & Stephen 2008). The stellar parameters of each probable stellar source in our test fields are identified by matching the de-reddened observed optical colours  $(g - i)_0$ ,  $(g - r)_0$  and  $(r - i)_0$ , with the synthetic colours. We applied a constant reddening for

**Table 2.** Summary of the results from the three test fields, when the black body model from S12 is used. The columns in the table represent the test field, NIR band for which the magnitudes are computed, the optical band used for the calculation of the scaling factor, total number of sources for which NIR observations were available to compare with the computed NIR magnitudes (M), the number of sources for which we could compute the NIR magnitudes within 0.3 mag with the observed NIR magnitudes (M1), the mean difference between the observed and the computed magnitudes ( $\delta m_{\text{mean}}$ , when sources within three times the error in the difference between the computed and observed magnitudes are considered), the standard deviation ( $\delta s$ ), and the percentage of outliers (M2, the sources which show a difference larger than 3 times the error in the difference between the observed and computed magnitudes). Note that for the test fields T1 and T3 the validation of the methodology is only up to  $J_{\text{Vega}} = 20$  mag. For T2, there is no H band observations to verify the method.

Test field	NIR band	Scaling factor	M	M1	$\delta m$	$\delta s$	M2
T1	J	<i>g</i>	868	768	-0.03	0.1	100
		<i>r</i>	868	779	-0.05	0.08	89
		<i>i</i>	868	875	-0.04	-0.09	93
		Average	868	781	-0.04	0.08	87
T1	H	<i>g</i>	868	567	-0.23	0.1	301
		<i>r</i>	868	610	-0.26	0.08	258
		<i>i</i>	868	579	-0.24	0.09	289
		Average	868	591	-0.26	0.09	277
T1	Ks	<i>g</i>	868	683	-0.19	0.1	185
		<i>r</i>	868	719	-0.19	0.1	149
		<i>i</i>	868	700	-0.23	0.09	168
		Average	868	694	-0.21	0.09	174
T2	J	<i>g</i>	3695	2652	-0.01	0.11	1043
		<i>r</i>	3695	2695	-0.06	0.1	1000
		<i>i</i>	3695	2746	-0.1	0.1	949
		Average	3695	2746	-0.05	0.09	949
T2	Ks	<i>g</i>	3695	2187	-0.03	0.12	1508
		<i>r</i>	3695	2297	-0.09	0.11	1398
		<i>i</i>	3695	2291	-0.13	0.13	1404
		Average	3695	2276	-0.09	0.12	1419
T3	J	<i>g</i>	2013	1735	-0.08	0.1	278
		<i>r</i>	2013	1755	-0.11	0.08	258
		<i>i</i>	2013	1770	-0.1	0.08	243
		Average	2013	1752	-0.09	0.09	261
T3	H	<i>g</i>	2013	1088	-0.21	0.11	925
		<i>r</i>	2013	1100	-0.23	0.1	913
		<i>i</i>	2013	1114	-0.22	0.8	899
		Average	2013	1108	-0.22	0.09	905
T3	Ks	<i>g</i>	2013	1213	-0.1	0.12	800
		<i>r</i>	2013	1252	-0.16	0.12	761
		<i>i</i>	2013	1190	-0.14	0.11	823
		Average	2013	1228	-0.15	0.1	785

all the sources, taken from map towards each test field (Schlegel *et al.* 1998). Due to the reasons that the synthetic colours are in the SDSS system and also the extinction co-efficients for the Mega Prime filters are not available, the observed Mega Prime colours and magnitudes are converted to SDSS system using the relations given in Gwyn & Stephen (2008). The extinction co-efficients for the SDSS system are taken from (Girardi *et al.* 2004, also refer S12). The sources whose three optical colours match with the model generated synthetic colours within 0.01 mag are considered. If there are multiple models identified for a single source with this condition,

then the model which show minimum deviation between the observed and synthetic colours is taken. The value 0.01 mag is the lower limit of the errors in the observed colours. We took this value to check whether we would get enough sources with this selection criterion.

Once the appropriate stellar model with parameters, temperature,  $\log(g)$  and metallicity is identified, then the magnitudes at the stellar surface in  $g$ ,  $r$ ,  $i$ ,  $J$ ,  $H$ ,  $Ks$  bands are used for further analysis. The observed optical magnitudes are compared with the model magnitudes and the scaling factor is estimated from each optical band. The average value of these three scaling factors is used to convert the JHKs magnitudes in Vega system to the apparent magnitudes. These apparent magnitudes are reddened and then compared with the observed JHKs magnitudes in Vega system for the validation of the methodology adopted.

#### 4.2 Application of methodology based on stellar atmospheric models

The above mentioned modified methodology is applied in the three test fields. In T1, there are 1882 probable stellar sources identified using the criteria  $17 \text{ mag} < I_{AB} < 21 \text{ mag}$  and half-light radius  $< 0.5 \text{ arcsec}$ . When NextGen model was used only 271 sources out of 1882, satisfied the selection criterion. Similarly we obtained only 248 sources when Kurucz template was used. The lower-left and lower-right panels in Fig. 10 show the difference between the computed and observed magnitudes when NextGen and Kurucz models are used and they are plotted against the observed  $J_{Vega}$  magnitude. The upper-left panel in Fig. 10 shows the difference between the observed and computed  $J_{Vega}$  magnitudes, when black body model was used. Also, out of 1882 sources, temperature could be estimated for only 868 sources. The upper-right panel shows the histograms of the difference between the observed and computed magnitudes when the stellar atmospheric models (NextGen and Kurucz) and the black body model are used to compute the  $J_{Vega}$  magnitude. Figures 11 and 12 are similar plots for the  $H_{Vega}$  and  $Ks_{Vega}$  bands respectively.

The results of all the tests based on stellar atmospheric models are given in Table 3. From Figures 10, 11 and 12, and Table 3, we can see that the difference between the observed and computed magnitudes (especially in the case of  $H_{Vega}$  and  $Ks_{Vega}$  magnitudes), reduces when the stellar atmospheric models are used. The number of outliers, which are sources which show a difference between the observed and computed magnitudes  $>$  three times the error is also reduced when stellar atmospheric models are used. But the number of sources (248 and 271 sources) which satisfied the selection criterion (observed and synthetic colours should match within 0.01 mag) are less. In the case of black body model, the number of sources for which we could compute the NIR magnitudes depend only on the initial colour–temperature relation. If we could estimate the temperature from the optical colour of the source, we can estimate the expected NIR magnitudes using the black body model. But in the case of stellar atmospheric models, the number of sources depends on the grid size of the parameters. In order to increase the number of sources, we need to decrease the grid spacing in temperature in the model templates and also specify a more realistic selection criterion for obtaining a model corresponding to a source. This is dealt within detail in sub-section 4.3.

In order to test the methodology based on stellar atmospheric models, a similar exercise was done to the 6262 sources which are identified as probable stellar sources

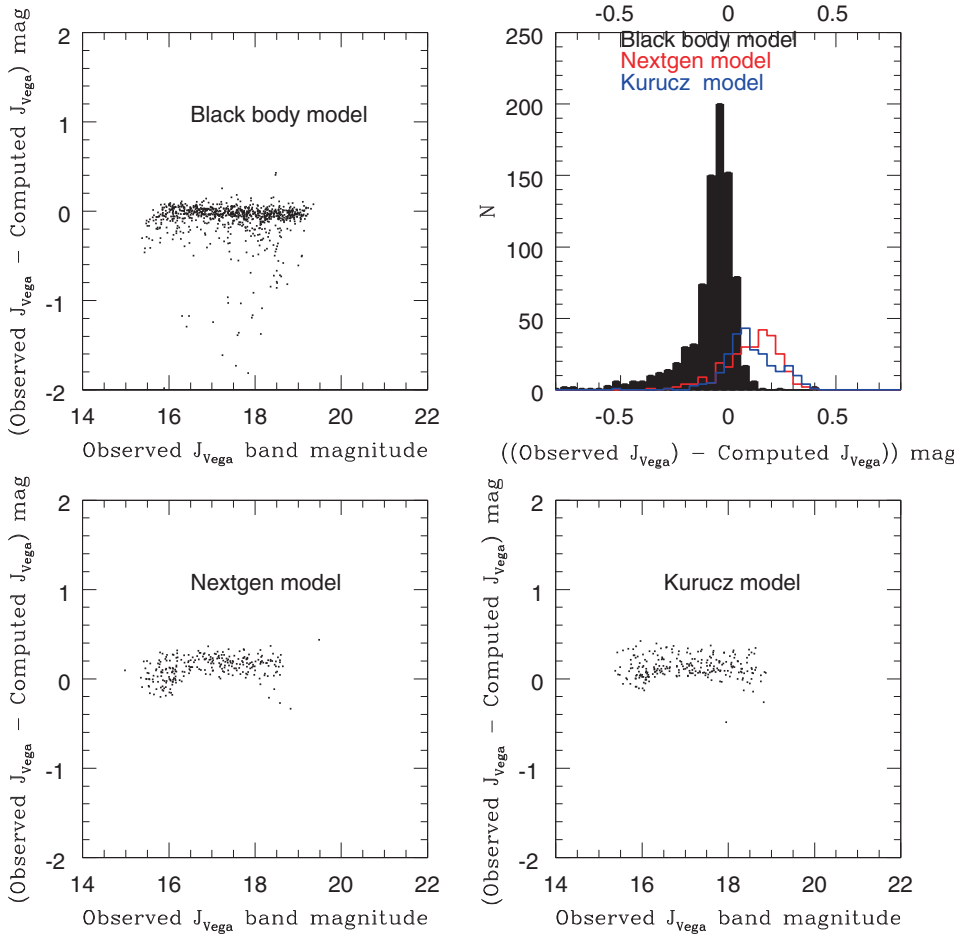


**Figure 10.** For the probable stellar sources in the test field, T1, the difference between the observed and computed magnitudes are plotted against the observed  $J_{Vega}$  magnitude. The models used are given in the respective panels. The upper-right panel shows the histogram of the difference between the observed and computed magnitudes for the three cases.

in the test field, T3. Out of 6262 sources we obtained a corresponding model for 1441 and 1361 sources from NextGen and Kurucz models respectively. When black body model was used, out of 6262 sources, temperature could be estimated for only 2013 sources. The number of sources obtained from Kurucz model is less compared to the NextGen model. This may be due to the large grid spacing in temperature in the Kurucz model. Even though the number of sources matched with NextGen model is large compared to Kurucz model, they are not sufficient to satisfy the source density criteria of TMT IRGSC. Even the number of sources for which we could estimate the NIR magnitudes using black body model is not sufficient. The fainter sources ( $I_{AB} > 21$  mag) need to be included to satisfy the source density criteria. Also by making the temperature grid spacing finer we can increase the source density in the test fields.

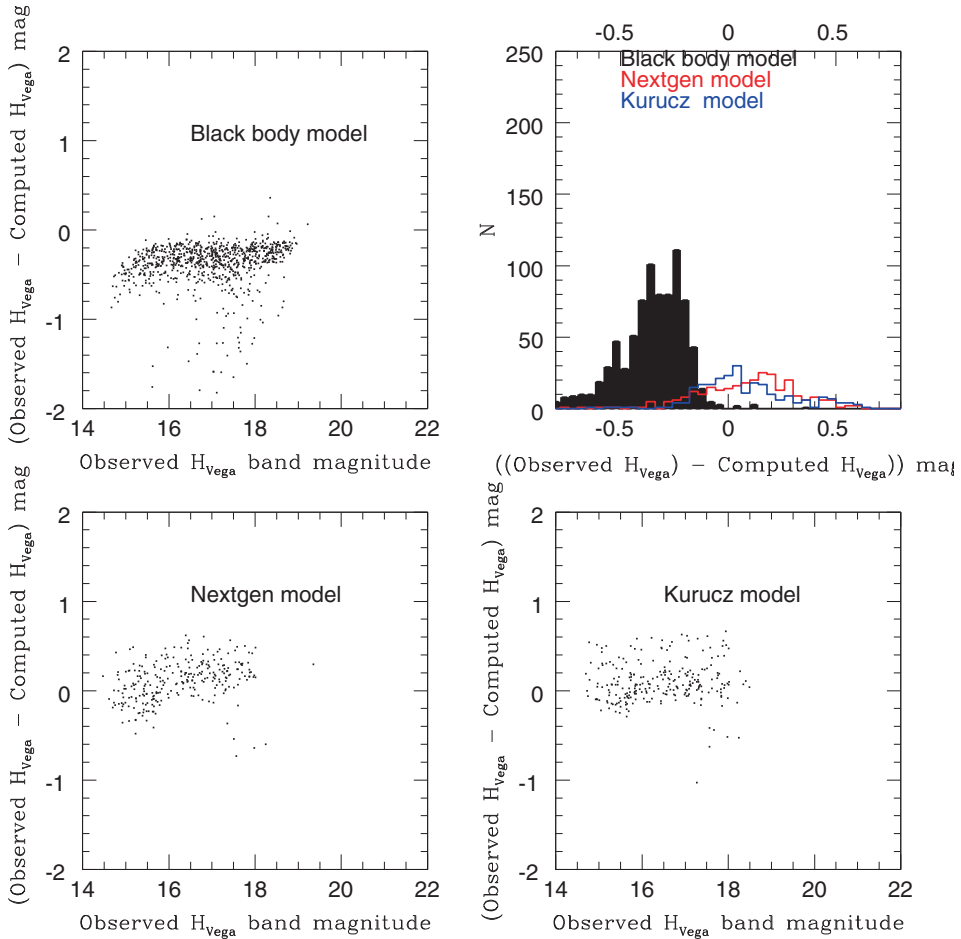


**Figure 11.** For the probable stellar sources in the test field, T1, the difference between the observed and computed magnitudes are plotted against the observed  $H_{Vega}$  magnitude. The models used are given in the respective panels. The upper-right panel shows the histogram of the difference between the observed and computed magnitudes for the three cases.

Figures 13, 14 and 15 are for the sources in the test field, T3 and are similar to Figures 10, 11 and 12. From the figures we can clearly see that difference between the observed and computed magnitudes reduces when stellar atmospheric models are used. The number of outliers (which show a difference between the observed and computed magnitudes greater than 0.3 mag) also decreases significantly. When Kurucz model is used, the difference between the observed and computed magnitudes in all the three NIR bands is nearly zero. This can be clearly seen from Table 3 and also the upper-right panel plot in Figures 13, 14 and 15. Also the dispersion is less for Kurucz model compared to other models. Thus we can say that Kurucz model is the better model to incorporate in the methodology for the computation of NIR magnitudes compared to NextGen model.

For the test field, T2 we had extended the star/galaxy classification criteria based on half-light radius till  $I_{AB} = 23$  mag. The number of sources identified using the

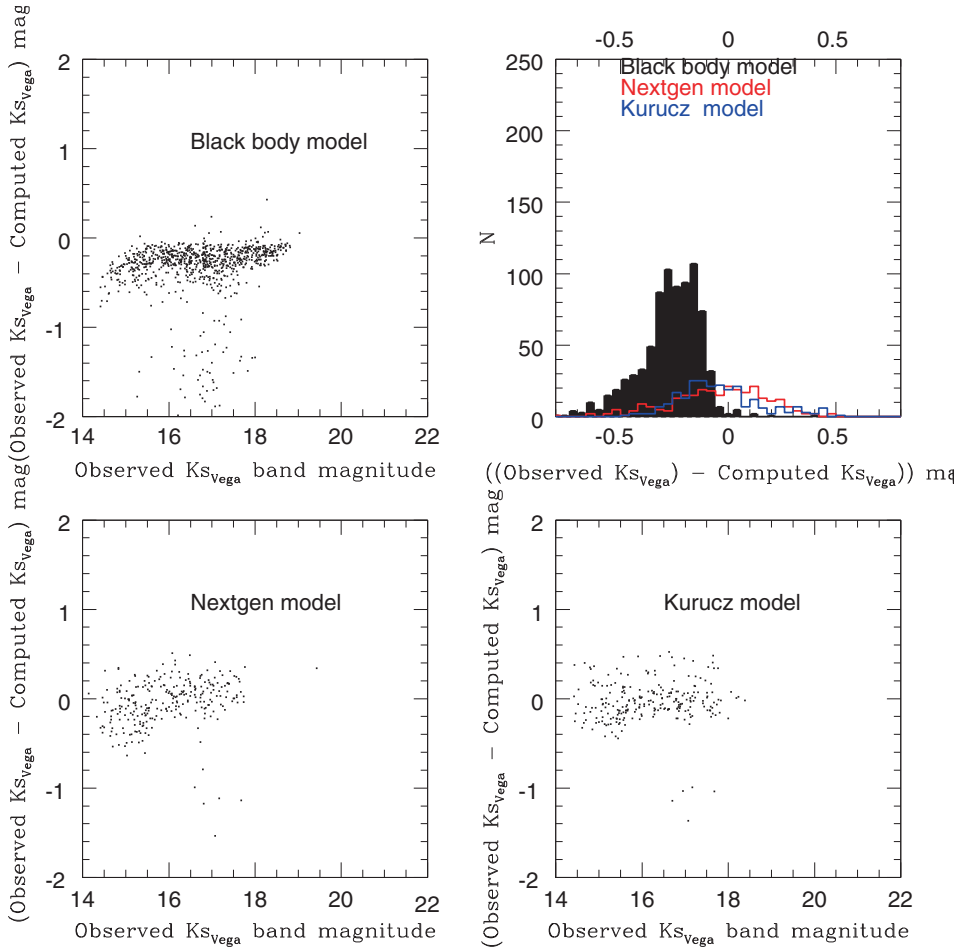


**Figure 12.** For the probable stellar sources in the test field, T1, the difference between the observed and computed magnitudes are plotted against the observed  $K_{s_{\text{Vega}}}$  magnitude. The models used are given in the respective panels. The upper-right panel shows the histogram of the difference between the observed and computed magnitudes for the three cases.

extended criteria is 9298. Out of 9298 sources we obtained a corresponding model for 3010 and 1979 sources from the NextGen and Kurucz models respectively. We applied the modified methodology to these sources. When black body model was applied we could estimate the temperature for 3695 sources. Even after extending the star/galaxy classification to fainter magnitudes, the number of sources for which the NIR magnitudes can be computed is not sufficient to satisfy the source density criteria of TMT IRGSC. This issue has to be looked carefully. As there is no observations in the H band for the sources in T2, we cannot compare the observed and computed H band magnitudes of sources in T2. Figures 16 and 17 are for the sources in the test field, T2 with extended star/galaxy classification and are similar to Figures 13 and 15. From the figures it is clearly seen that when stellar atmospheric models are used, the outliers decrease significantly. Also it is seen that the Kurucz model is better for the computation of NIR magnitudes.

**Table 3.** Summary of the results from three test fields, when stellar atmospheric models (before interpolation) are used in comparison with the black body model (when the average of value scaling factor is used). The columns in the table represent the test field, NIR band for which the magnitudes are computed, the model used, total number of probable stellar sources identified from the optical catalog, total number of sources for which we could estimate the NIR magnitudes (M), the number of sources for which we could compute the NIR magnitudes within 0.3 mag with the observed NIR magnitudes (M1), the mean difference between the observed and the computed magnitudes ( $\delta m_{\text{mean}}$ , when sources within 3 times the error of the difference between the observed and computed magnitudes are considered and here the average error in the computed magnitude is  $\sim 0.1$  mag), the standard deviation ( $\delta s$ ), and the percentage of outliers (M2, the sources which show a difference larger than 3 times the error). Note that for the test fields T1 and T3 the validation of the methodology is only up to  $J_{\text{Vega}} = 20$  mag. For T2 there is no H band observations to verify the method.

Test field	NIR band	Model	N	M	M1	$\delta m$	$\delta s$	M2
T1	J	Black body	1882	878	781	-0.04	0.08	87 (10%)
		Kurucz	1882	248	223	0.02	0.02	25 (1%)
		NextGen	1882	271	244	0.05	0.12	27 (%)
T1	H	Black body	1882	878	591	-0.26	0.09	277 (32%)
		Kurucz	1882	248	198	0.04	0.12	50 (20%)
		NetGen	1882	271	211	0.07	0.15	60 (22%)
T1	Ks	Black body	1882	878	694	-0.21	0.09	174 (21%)
		Kurucz	1882	248	213	-0.02	0.14	35 (6%)
		NextGen	1882	271	216	0.06	0.15	55 (8%)
T2	J	Black body	9298	3695	2746	-0.05	0.09	949 (27%)
		Kurucz	9298	1979	1939	-0.007	0.07	40 (2%)
		NextGen	9298	3010	2920	-0.01	0.1	90 (3%)
T2	Ks	Black body	9298	3695	2276	-0.09	0.12	1419 (34%)
		Kurucz	9298	1979	1939	0.02	0.12	376 (19%)
		NextGen	9298	3010	2588	-0.03	0.17	420 (14%)
T3	J	Black body	6262	2013	1752	-0.09	0.09	261 (13%)
		Kurucz	6262	1361	1279	0.02	0.09	82 (6%)
		NextGen	6262	1441	1325	-0.06	0.12	115 (8%)
T3	H	Black body	6262	2013	1108	-0.22	0.09	905 (45%)
		Kurucz	6262	1361	952	0.05	0.14	408 (30%)
		NextGen	6262	1441	1124	-0.04	0.16	317 (29%)
T3	Ks	Black body	6262	2013	1228	-0.15	0.1	785 (39%)
		Kurucz	6262	1361	940	0.05	0.13	421 (31%)
		NextGen	6262	1441	1124	-0.04	0.16	317 (22%)

From all the figures (Figures 10 to 17) and from Table 3, the important points to be noted are

1. The difference observed between the observed and computed magnitudes when black body model was used (especially in the H and Ks bands) is reduced when stellar atmospheric models are used. Especially when Kurucz model is used, the mean difference is around zero magnitude in NIR bands. But the scatter is slightly more in some cases. The scatter in the difference between the computed and observed magnitudes may be due the error propagated in the transformation of magnitudes and colours from one filter system to the other. Also the error in observed optical colours may be another reason. The scatter may also depend on the grid size in the model. Finer grid may help to reduce the scatter.
2. The number of outliers in the test field decreases significantly when stellar atmospheric models are used compared to that when black body was used. The sources

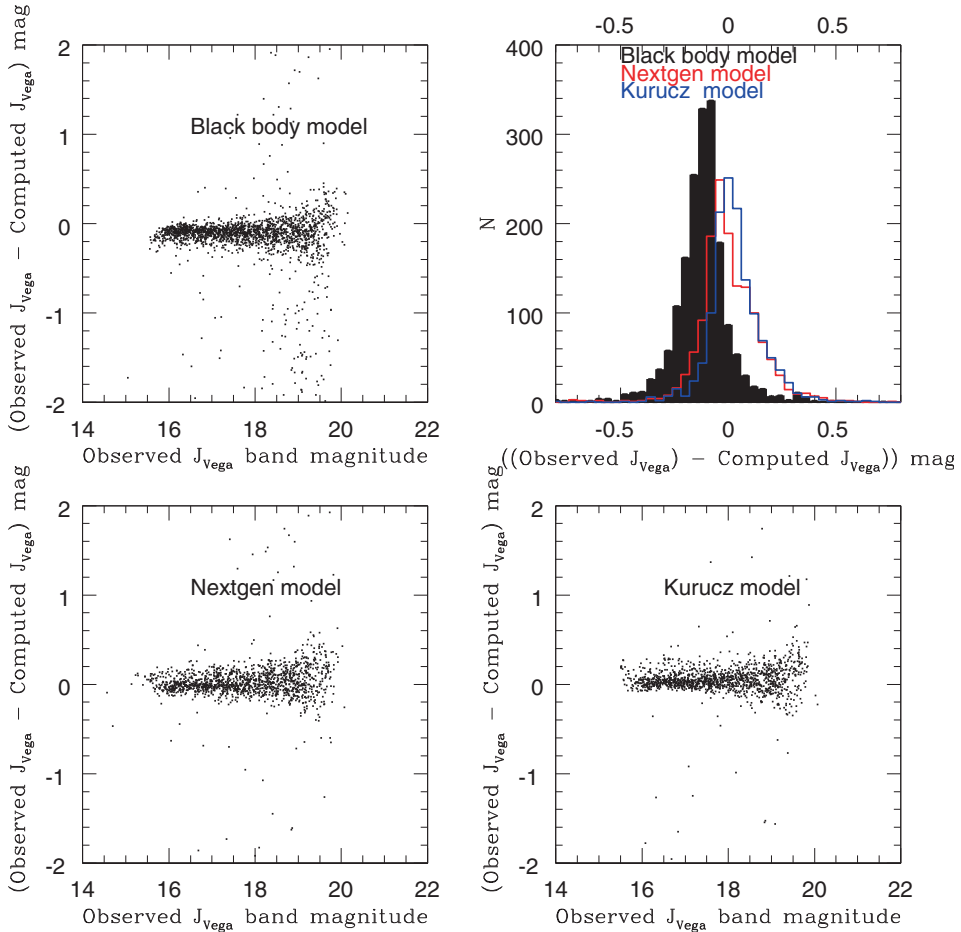


**Figure 13.** Same as Fig. 10, but for the test field T3.

removed may not be stars. The decrease in the number of outliers, suggest that matching the synthetic colours with the observed colours is a good tool to separate star/galaxy from the optical data. Figures 16 and 17 suggest that this method can be extended to the fainter optical magnitudes for optimal star/galaxy separation. If the star/galaxy criteria is extended to fainter optical magnitudes ( $I_{AB} \sim 23$  mag) then we can reach up to  $J_{Vega} = 22$  mag, which is one of the criteria of the TMT IRGSC.

3. The source density criteria of 3 stars per 2 arcmin field-of-view of NFIRAOS translates to a requirement that minimum 3440 sources should be there in 1 square degree field in the sky. This is not satisfied in the test fields used. Other than the test field, T1 the other two fields have enough optical sources to satisfy this requirement. But when the methodology is applied for the computation of NIR magnitudes, the number decreases. In order to increase the number of sources in the test field for which the NIR magnitudes can be computed from optical magnitudes, we need to make the temperature grid spacing of the model templates finer. This is very essential.

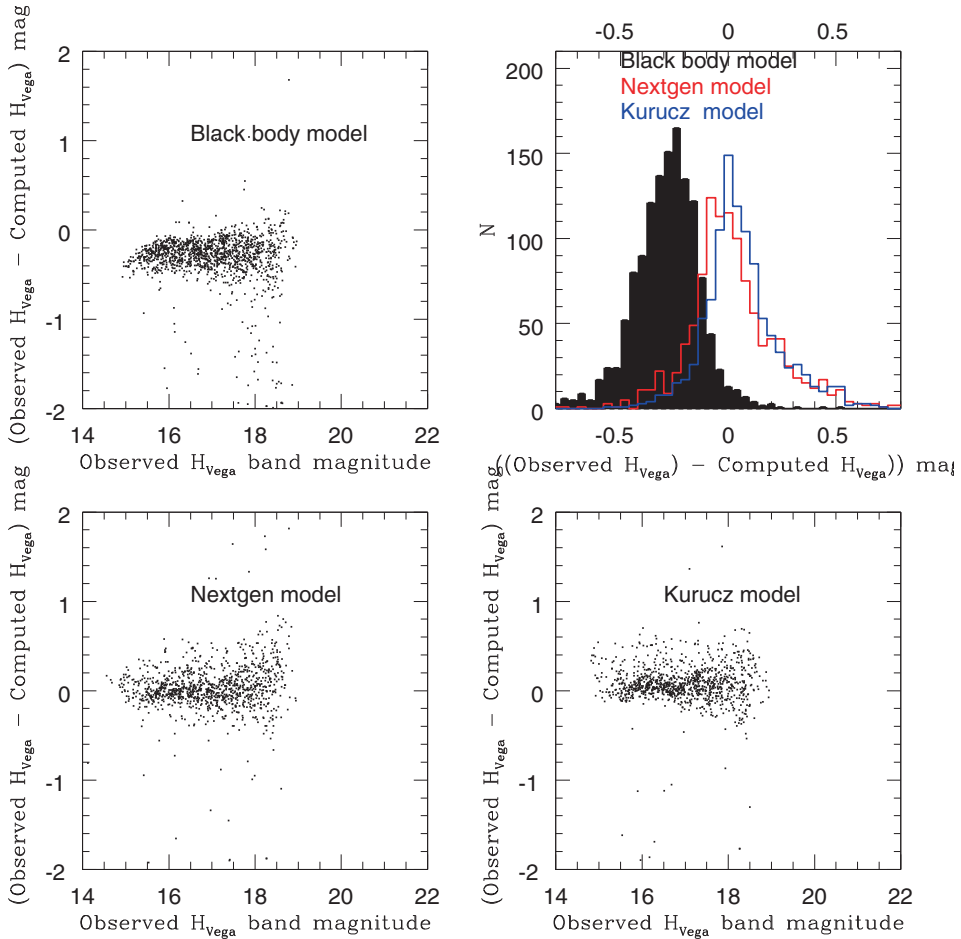


**Figure 14.** Same as Fig. 11, but for the test field T3.

#### 4.3 Interpolation of stellar models and its application

We created three interpolated models from the Kurucz model. One with a simple linear interpolation only in the effective temperature, with a grid size of 125 K and the second one with a linear interpolation in effective temperature, with a grid size of 62.5 K. Then we generated the third interpolated model by making the grid size finer in all the stellar atmospheric parameters (effective temperature grid size = 62.5 K,  $\log(g)$  grid size: 0.25, Fe/H grid size: 0.25) by simultaneous interpolation.

The parameter range and the grid size of the three interpolated models are given below:

*Model 1:*  $3500 < T_{\text{eff}} < 10000$  K, with grid size of 125 K for the whole range of temperature;  $0 < \log(g) < 6.0$ , with a grid size of 0.5 in  $\log(g)$ ;  $-4.0 < [\text{Fe}/\text{H}] < +0.0$ , with a grid size of 0.5 in Fe/H.

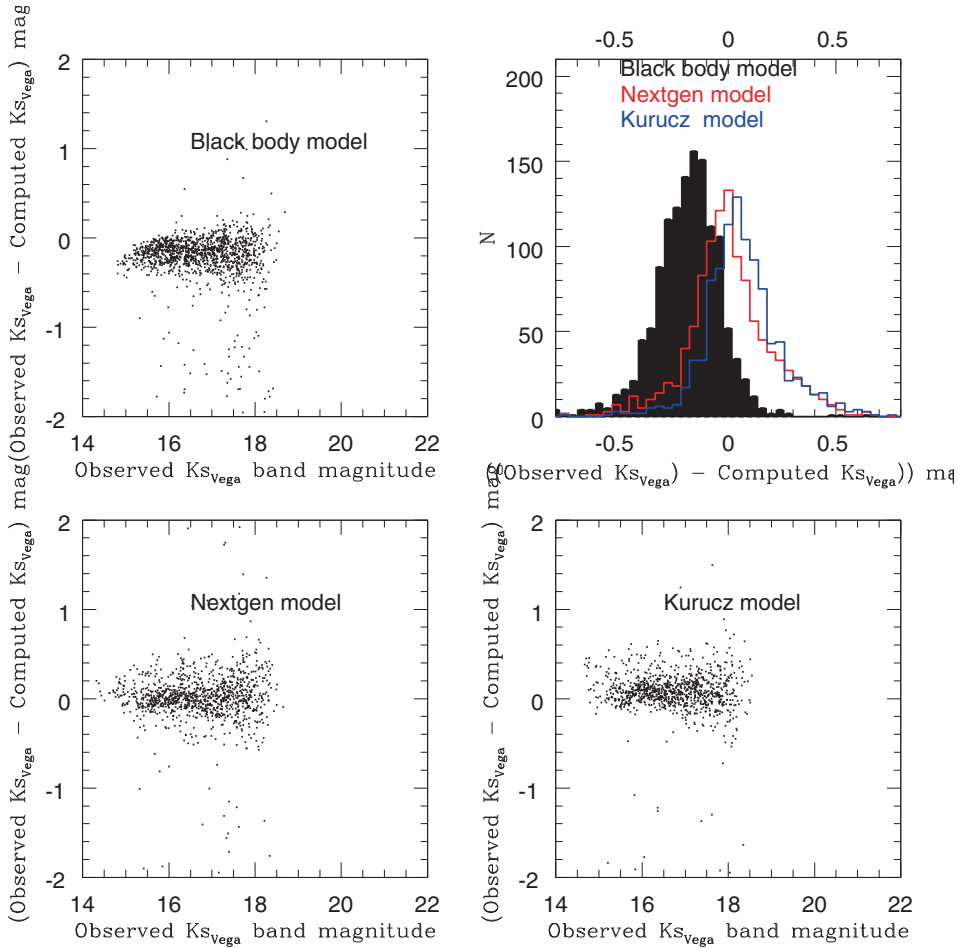


**Figure 15.** Same as Fig. 12, but for the test field T3.

*Model 2:*  $3500 < T_{\text{eff}} < 10000$  K, with a grid size of 62.5 K for the whole range of temperature;  $0 < \log(g) < 6.0$ , with a grid size of 0.5 in  $\log(g)$ ;  $-4.0 < [\text{Fe}/\text{H}] < +0.0$ , with a grid size of 0.5 in Fe/H.

*Model 3:*  $3500 < T_{\text{eff}} < 10000$  K, with a grid size of 62.5 K for the whole range of temperature;  $0 < \log(g) < 6.0$ , with a grid size of 0.25 in  $\log(g)$ ;  $-4.0 < [\text{Fe}/\text{H}] < +0.0$ , with a grid size of 0.25 in Fe/H.

The interpolated models are used in the methodology to compute NIR magnitudes. The application in the test field, T2 (for which we have observed NIR data till  $J_{\text{Vega}} = 22$  mag for the validation) and fine tuning based on the results are described below.

Initially the methodology incorporating Model 1 (the decrease in grid spacing in temperature by half, from 250 K to 125 K) is applied to the sources in test field T2. The incorporation of realistic error in the identification of the appropriate stellar atmospheric model, by matching the de-reddened observed colour and synthetic

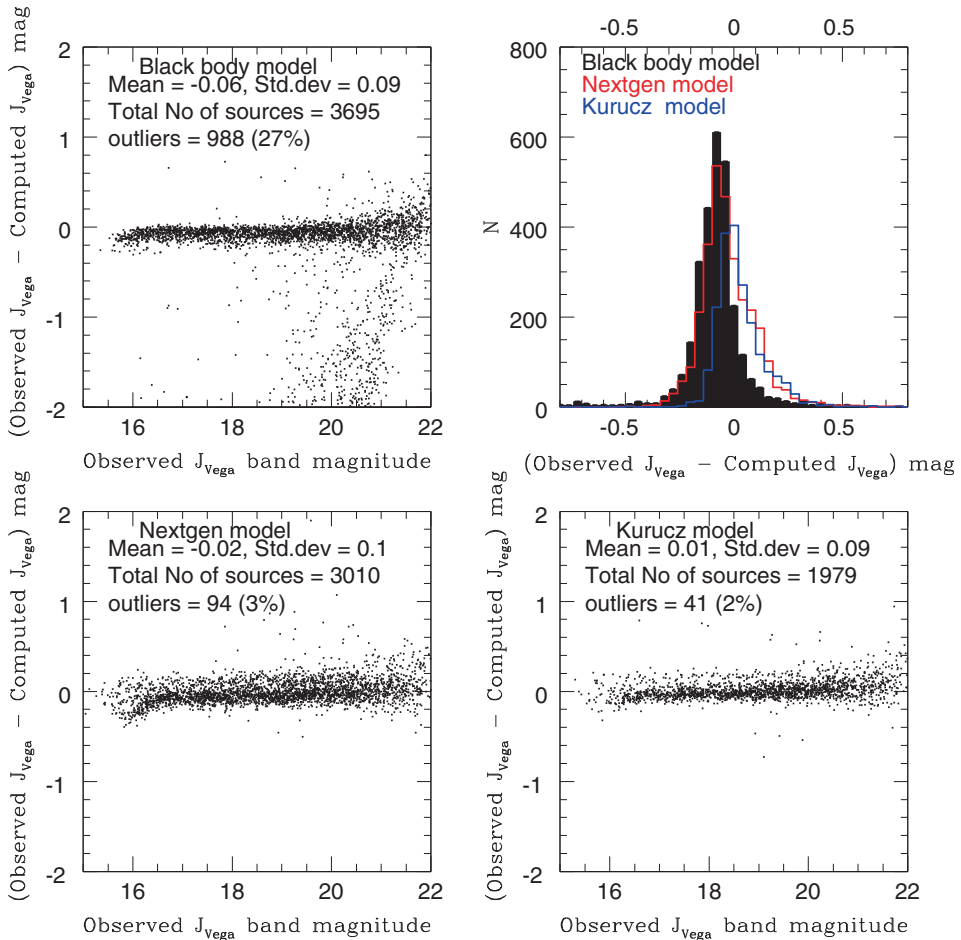


**Figure 16.** Same as Fig. 14 but for the test field T2, with extended star/galaxy classification applied for the selection of probable stellar sources from the optical catalog.

colour, for the source is considered. The lower and upper limits of the observed error in the magnitude range,  $i = 17$  to 23 mag are 0.01 and 0.04 respectively. Corresponding upper limits of error in the  $g$  and  $r$  bands are 0.02 and 0.03 respectively. One of the requirements of the TMT IRGSC is that the error in the NIR magnitudes should be  $\leq 0.2$  mag. This requirement sets the upper limits of the observed errors, the criteria to chose the cut off value for the matching of observed and synthetic colours. Based on error propagation rule, the upper limits of observed magnitudes translate into an error of  $\sim 0.05$  mag in the computed NIR magnitudes. This error of 0.05 mag is mostly associated with the fainter magnitudes. If we consider two times error in the observed magnitudes as the criteria, then the propagated error associated with the fainter computed magnitudes would be  $\sim 0.11$  mag. Similarly if we consider three times the observed errors as the criteria, the propagated error associated with the fainter computed magnitudes would be  $\sim 0.16$  mag. So in principle, we can use 3 times the observed errors as the criteria for identification of the appropriate

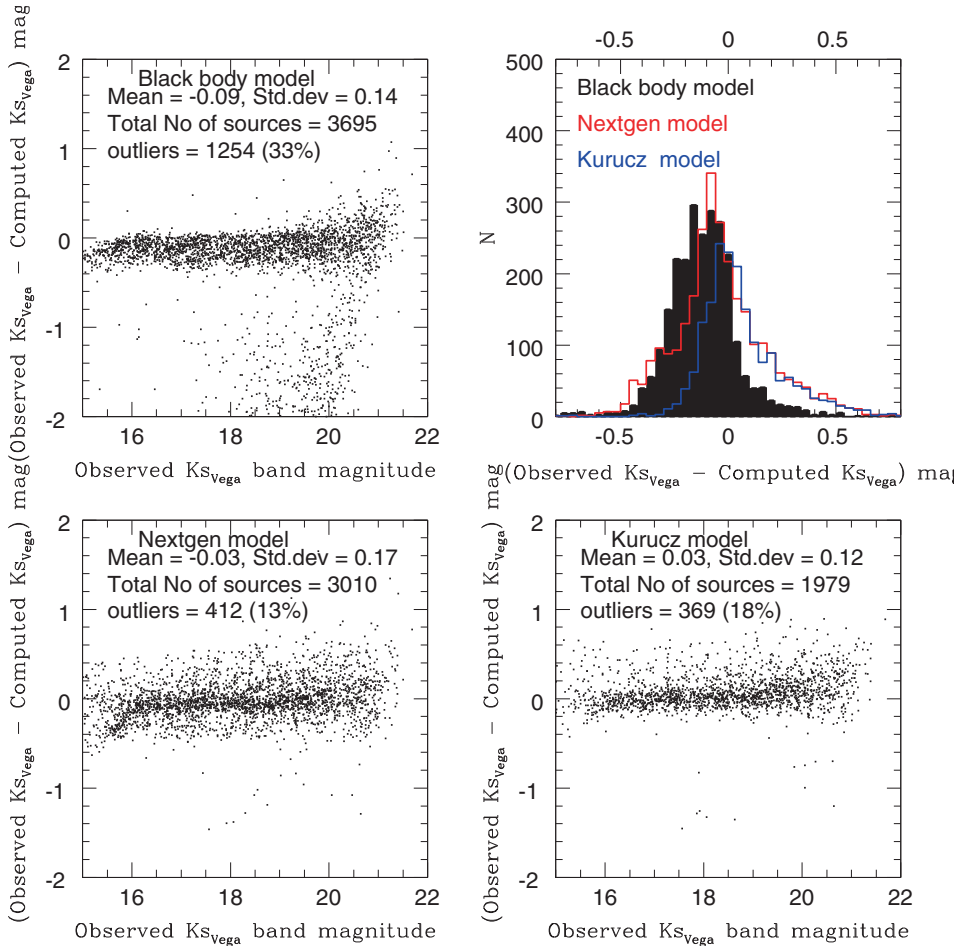


**Figure 17.** Same as Fig. 16 but for the test field T2, with extended star/galaxy classification applied for the selection of probable stellar sources from the optical catalog.

model for the computation of the NIR magnitudes. But these errors, associated with the computed magnitudes, mentioned above are estimated only considering the observed errors in the optical magnitudes and their propagation in the calculation of the NIR magnitudes. The errors associated with the synthetic colours and model generated magnitudes are not considered as they are not given in the models. So we need to leave some margin for the errors contributed from the synthetic magnitudes and synthetic colours. Thus it is safe to use 2 times the observed errors as the criteria for the identification of the model. When stellar atmospheric models were used before interpolation (section 4.2), the criterion for selection of models corresponding to sources was a fixed value of 0.01 mag, which was the lower limit of the errors in the observed colours. This was not realistic, especially in the case of fainter objects which had larger errors for their observed magnitudes and hence their observed colours. Now in the application of interpolated stellar atmospheric models, we changed this criteria to a more realistic value, which is 2 times the error in the

observed colour of each source. This revised criteria along with interpolated models would help to retrieve more sources from the optical catalog for which we could estimate the NIR magnitudes.

Model 1 is used for the computation of NIR magnitudes with a criteria of two times the observed errors for the identification of the appropriate model for the source. The number of retrieved sources from the optical catalog, for which NIR magnitudes are computed, increased (3995 sources in one  $\text{deg}^2$  field) and the number was enough to satisfy the source density criteria of NFIRAOS. Hence in test field, T2 the source density criteria of NFIRAOS is satisfied. The sources in the magnitude range 16–22 mag in  $J_{\text{Vega}}$  band are obtained. Thus the application of the interpolated Kurucz model (making the temperature grid spacing finer) and the incorporation of the realistic errors (2 times the observed errors in colours) in the criteria for the retrieval of the sources are needed to satisfy the source density criteria of NFIRAOS. In order to validate the computation of NIR magnitudes using the interpolated model, we compared the computed NIR magnitudes with the observed NIR magnitudes which are available from UKIDSS survey. The lower left and upper left panels of Fig. 18 show the difference in the observed and computed magnitudes plotted against the observed magnitude. From the plot, we can see that there are two sequences, one which has a mean difference of zero (shown as red points) and another parallel sequence (shown as black points) with mean difference of  $\sim 0.2$  mag in the  $J_{\text{Vega}}$  band and a mean difference of  $\sim 0.5$  mag in the Ks band. Thus one sequence has sources with similar observed and computed magnitudes and the parallel second sequence has sources with computed magnitudes brighter than the observed magnitudes. The sources with computed magnitudes brighter than the observed magnitudes constitute  $\sim 30\%$  of the retrieved sources and these sources are identified as those for which the model temperature is less than 4000 K and  $\log(g) < 3$ . These sources are shown as black points in Fig. 18.

We applied the methodology incorporating Model 2 (with temperature grid spacing of 62.5 K) to the sources in the test field T2, with the criteria of 2 times the observed errors in colours as the criteria for matching the synthetic and observed colours. The number of sources retrieved are 4480 which is sufficient to satisfy the source density criteria of NFIRAOS. But when the difference between the observed and computed magnitudes are plotted against the observed magnitudes, the two sequences are seen. This is illustrated in the upper right and lower right panels of Fig. 18. The black points are those which are identified as those for which the model temperature is less than 4000 K and  $\log(g) < 3$ . They constitute  $\sim 30\%$  of the retrieved sources.

Thus in the two cases described above, the computed magnitudes of the sources in the optical catalog which are identified as cooler giants from the matched model parameters are brighter than the observed magnitudes. Hence the stellar atmospheric models with temperature less than 4000 K and  $\log(g) < 3$  are not reliable for the computation of the NIR magnitudes from the optical sources. We consider only the stellar atmospheric models with  $T_{\text{eff}} \geq 4000$  K and also models in the temperature range 3500–4000 K with  $\log(g) \geq 3$  for the computation of NIR magnitudes. This reduces the number of sources retrieved from the optical sample  $\sim 2796$  and  $\sim 3136$  sources in the two cases described. These numbers are not sufficient to satisfy the source density criteria of the NFIRAOS.

Instead of making the temperature grid finer than 62.5 K we interpolated the  $\log(g)$  and Fe/H grid spacing. The initial spacing in the gravity and metallicity grids was

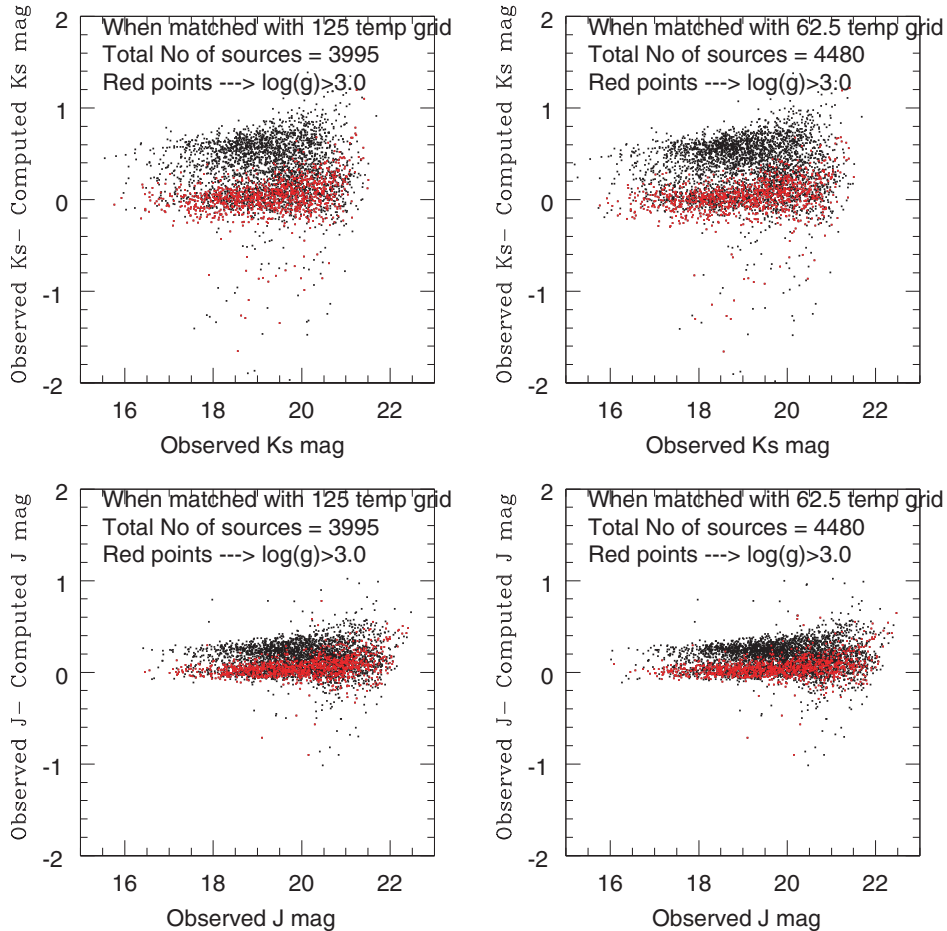


**Figure 18.** The difference between the observed and computed magnitudes are plotted against observed magnitudes for the sources in the test field, T2. The NIR magnitudes are computed using the interpolated Kurucz stellar atmospheric models with finer temperature grids. The temperature grid spacing is shown in the panels. The black points are those which are identified as sources with temperatures  $<4000$  K with  $\log(g) < 3$ .

0.5 dex. We made it finer to 0.25 dex in both the parameters and interpolated the model (Model 3). Model 3 is incorporated in the methodology for the computation of NIR magnitudes with a matching criteria of 2 times the observed errors in colours. The number of sources retrieved are 5065, with 30% of them corresponding to the model temperature 3500–4000 K and  $\log(g)$  less than 3. For these 30% sources, the computed NIR magnitudes are brighter than the observed NIR magnitudes. The remaining 70% (3546) are enough to satisfy the source density criteria of NFIRAOS. But only 38% of the total sources in the optical catalog are retrieved. Further interpolation of stellar atmospheric models to increase the number of retrieved sources is not feasible as we do not know the errors associated with the model parameters, and cannot make the grid spacing finer than the errors. We need to identify solutions by which we can estimate the NIR magnitudes of these 30% sources without discrepancy. The

different possibilities and identification of an optimal model is described in next section. The results of the test based on interpolated Kurucz model are given in Table 4.

### 5. Identification of an optimal model

The possible ways in which we tried to identify an optimal model are:

(a) *To find the second best model for the sources which show discrepancy:* This step is to identify the second best match model (corresponding to 30% sources which show discrepancy) from the model parameter range of temperature  $>4000$  K and temperature  $<4000$  K with  $\log(g) > 3$  and see whether the computed magnitudes are comparable with the observed magnitudes. The models corresponding to the temperature 3500–4000 K and  $\log(g) < 3$  are removed from the interpolated model parameter space and then applied to the sources in the test field, T2 with the same criteria of 2 times the observed error for the identification of the appropriate model. This resulted in the retrieval of 3790 sources, which are sufficient to satisfy the source density criteria of NFIRAOS. For more than 95% of these sources, the computed and the observed magnitudes are comparable. This is shown in Fig. 19. The lower panel shows the difference between the observed and computed magnitudes against the observed magnitudes. The upper panel shows the distribution of the difference between the observed and the computed magnitudes. From the plot we can see that the mean difference between the observed and the computed magnitudes is  $\sim 0$  in both the panels. The scatter is more in Ks bands, which was seen in all the previous cases. Previously, we saw that when the interpolated models of temperatures less than 4000 K with  $\log(g) < 3$  were included, 30% of the retrieved sources (1519/5065) were found to have discrepancy between their computed and observed NIR magnitudes. When the models with temperature  $<4000$  K with  $\log(g) < 3$  were excluded, we found that out of 30% outliers, 5% (244 sources) had second best match models (in the parameter range of temperature  $>4000$  K and temperature  $>3500$  K with  $\log(g) > 3$ ) which were good enough to reproduce the observed magnitudes. Thus we can say that the Kurucz interpolated stellar atmospheric models with temperatures  $>4000$  K and  $<3500$  K and  $\log(g) > 3$  can be used for the computation of the NIR magnitudes of stellar sources from their optical magnitudes.

The test field, T2 have 9298 sources which are classified as stars based on the extended half-light radius criteria. Out of these 9298 sources only 3790 sources are retrieved for which the NIR magnitudes are estimated. Though the source density criteria of NFIRAOS is satisfied for the test field, T2, there are many sources in the optical catalog for which an appropriate model was not found and hence could not estimate the NIR magnitudes of these sources. As mentioned earlier, further interpolation of the models is not physically feasible as the grid spacing cannot be made further finer without the information on the errors associated with the models. Also, even if further interpolation of models with temperatures  $>4000$  K is carried out, the increase in the number of sources shall be marginal. This is because most of the sources in the optical catalog which are not retrieved are mostly cooler sources for which the model estimates are not appropriate. This is the limitation of the stellar atmospheric model. Another way to increase the number of sources for which we can get an appropriate model is to increase the criteria for the identification of the model to 3 times the observed errors in colour. This increases the errors associated

**Table 4.** Summary of the results from T2, when the interpolated stellar models are used. The columns in the table represent the test field, NIR band for which the magnitudes are computed, interpolation model used, total number of probable stellar sources from the optical catalog (N), the number of sources for which we could compute NIR magnitudes (M), comments for the test fields T1 and T3 that the validation of the methodology is only up to  $J_{\text{Vega}} = 20$  mag. For T2 there is no H band observations to verify the method.

Test field	NIR band	Interpolated model	N	M	Comments on the (observed - computed) magnitude distribution
T2	J	Model 1	9298	3995	Two peaks: $\sim 0.0$ mag (70% of the sources) and $\sim 0.2$ mag (30% of the sources)
T2	J	Model 2	9298	4480	Two peaks: $\sim 0.0$ mag (70% of the sources) and $\sim 0.2$ mag (30% of the sources)
T2	J	Model 3	9298	5065	Two peaks: $\sim 0.0$ mag (70% of the sources) and $\sim 0.2$ mag (30% of the sources)
T2	Ks	Model 1	9298	3995	Two peaks: $\sim 0.0$ mag (70% of the sources) and $\sim 0.5$ mag (30% of the sources)
T2	Ks	Model 2	9298	4480	Two peaks: $\sim 0.0$ mag (70% of the sources) and $\sim 0.5$ mag (30% of the sources)
T2	Ks	Model 3	9298	5065	Two peaks: $\sim 0.0$ mag (70% of the sources) and $\sim 0.5$ mag (30% of the sources)
T2	J	Model 1 with $T_{\text{eff}} > 4000$ K and with $3500 \text{ K} \leq T_{\text{eff}} \leq 4000$ K and $\log(g) \leq 3$	9298	2797	Single peak at $\sim 0.0$ mag
T2	J	Model 2 with $T_{\text{eff}} > 4000$ K with $3500 \text{ K} \leq T_{\text{eff}} \leq 4000$ K and $\log(g) \leq 3$	9298	3136	Single peak at $\sim 0.0$ mag
T2	J	Model 3 with $T_{\text{eff}} > 4000$ K with $3500 \text{ K} \leq T_{\text{eff}} \leq 4000$ K and $\log(g) \leq 3$	9298	3790	Single peak at $\sim 0.0$ mag
T2	Ks	Model 1 with $T_{\text{eff}} > 4000$ K with $3500 \text{ K} \leq T_{\text{eff}} \leq 4000$ K and $\log(g) \leq 3$	9298	2797	Single peak at $\sim 0.0$ mag
T2	Ks	Model 2 with $T_{\text{eff}} > 4000$ K with $3500 \text{ K} \leq T_{\text{eff}} \leq 4000$ K and $\log(g) \leq 3$	9298	3136	Single peak at $\sim 0.0$ mag
T2	Ks	Model 3 with $T_{\text{eff}} > 4000$ K with $3500 \text{ K} \leq T_{\text{eff}} \leq 4000$ K and $\log(g) \leq 3$	9298	3790	Single peak at $\sim 0.0$ mag
T2	J	Combined model, Model 3 with $T_{\text{eff}} > 4000$ K with interpolated NextGen model with $T_{\text{eff}} \leq 4000$ K	9298	7077	Single peak at $\sim 0.08$ mag
T2	Ks	Combined model, Model 3 with $T_{\text{eff}} > 4000$ K with interpolated NextGen model with $T_{\text{eff}} \leq 4000$ K	9298	7077	Single peak at $\sim 0.12$ mag

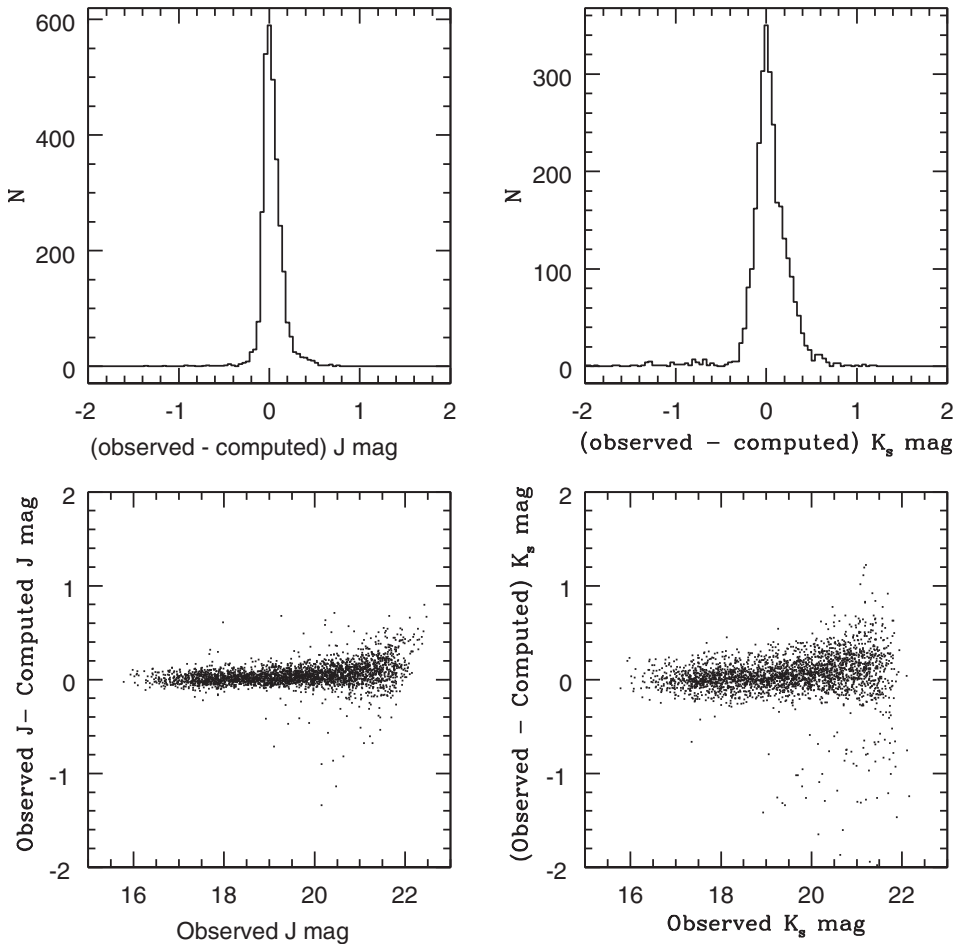


**Figure 19.** The difference between the observed and computed magnitudes are plotted against observed magnitudes for the sources in the test field, T2. The NIR magnitudes are computed using the interpolated Kurucz stellar atmospheric models with temperatures  $>4000$  K and  $<3500$  K, and  $\log(g) > 3$ .

with the computed NIR magnitudes of the fainter sources and this error (0.16 mag) is close to the maximum error criteria of the guide stars. Though the error is large, we can still consider this as a possibility to increase the number of sources for which NIR magnitudes can be computed. When we considered 3 times the observed errors in colour as the criteria for the identification of the appropriate model, the number of sources increased, but only marginally. This is mainly because of the fact that the non retrieved sources are mostly cooler objects and the models are not good enough in the cooler temperature range. So we need to adopt some methods to include the cooler sources.

(b) *Including the NextGen stellar atmospheric models for the computation of the NIR magnitudes of cooler stars:* From the analysis in section 4, we found that the Kurucz model is better than NextGen model for the computation of NIR magnitudes.

Though Kurucz was found better, NextGen also could compute the NIR magnitudes with reliable accuracy. Also, as the NextGen model has a lower temperature limit of 2700 K in comparison with that of the Kurucz model of 3500 K, we can try this model for solving the discrepancy of cooler stars. The mismatch between the computed magnitudes and observed magnitudes can be attributed as the limitation of the Kurucz model in the cooler temperature range. The NextGen model uses opacities due to dust formation which is important for cool stars. As the NextGen model has a lower temperature limit up to 2700 K, we tried using the NextGen model in the temperature range 2700–4000 K, combined with the interpolated Kurucz models, above 4000 K. The temperature grid spacing of the original NextGen model is 100 K. So we combined the NextGen model in the temperature range 2800–4000 K (without any interpolation) with the Model 1 (interpolated Kurucz model with temperature grid spacing of 125 K) above a temperature of 4000 K. The combined model was applied to the sources in the test field, T2 with the 2 times observed error as the criteria for the identification of the appropriate model and hence the computation of the NIR magnitudes. This resulted in the retrieval of 6154 sources. The number of retrieved sources increases and they are enough to satisfy the source density criteria of NFIRAOS. The two sequences which we observed in the previous cases are not very prominent when NextGen models are used in the cooler temperature regime. But there are a few outliers, whose observed and computed magnitudes are not comparable and the discrepancy was very large. Those sources are identified as sources with temperature less than 3000 K. So for the final model for the computation of NIR sources from the optical sources consist of Kurucz models ( $T > 4000$  K) and the NextGen models ( $3000 \text{ K} < T < 4000 \text{ K}$ ). Figure 20 shows the difference plots (in  $J_{\text{Vega}}$  band) and the histogram of the retrieved sources in the test field, T2 with Kurucz model alone and with the combined model of Kurucz and NextGen. From the upper left and upper right panels which show the histogram of the difference in the observed and computed magnitudes, we can clearly see that the observed two sequences are merged to one in the case when the combined model is used. The H and Ks band magnitudes are also compared for the other test fields and Ks band magnitudes are tested for the sources in the test field, T2. The plot similar to Fig. 20, for the Ks band is shown in Fig. 21. From Fig. 21 also, we can see that the two sequences observed with interpolated Kurucz models, are not there when the combined model is used. The histogram also shows a single peak. This suggests that the combined model of Kurucz models and NextGen models can be used as an optimal model for the computation of the NIR magnitudes from optical sources. The retrieved sources constitute 66% of the total sources in the optical catalog. Out of the these 66%, a few stars ( $\sim 6\%$ ) show large deviation (deviation  $> 0.3$  mag, which is  $\sim 3$  times the error in the computed magnitudes) between the observed and computed magnitudes. Thus  $\sim 60\%$  of the stars which are retrieved from the optical catalog can be used as guide stars. The remaining sources in the optical catalog are non-stellar sources, for which a stellar atmospheric model is not applicable. The histograms in the upper and right panels of Figures 20 and 21 show more number of sources with positive difference relative to zero and the peak is at  $\sim 0.2$  mag. This means that for a majority of sources the computed magnitudes are brighter by  $\sim 0.2$  mag in the case of both J and Ks magnitudes. In the case of Ks magnitudes, the difference between the observed and computed magnitudes show an asymmetric tail in the positive difference direction. These are discussed in the next section.

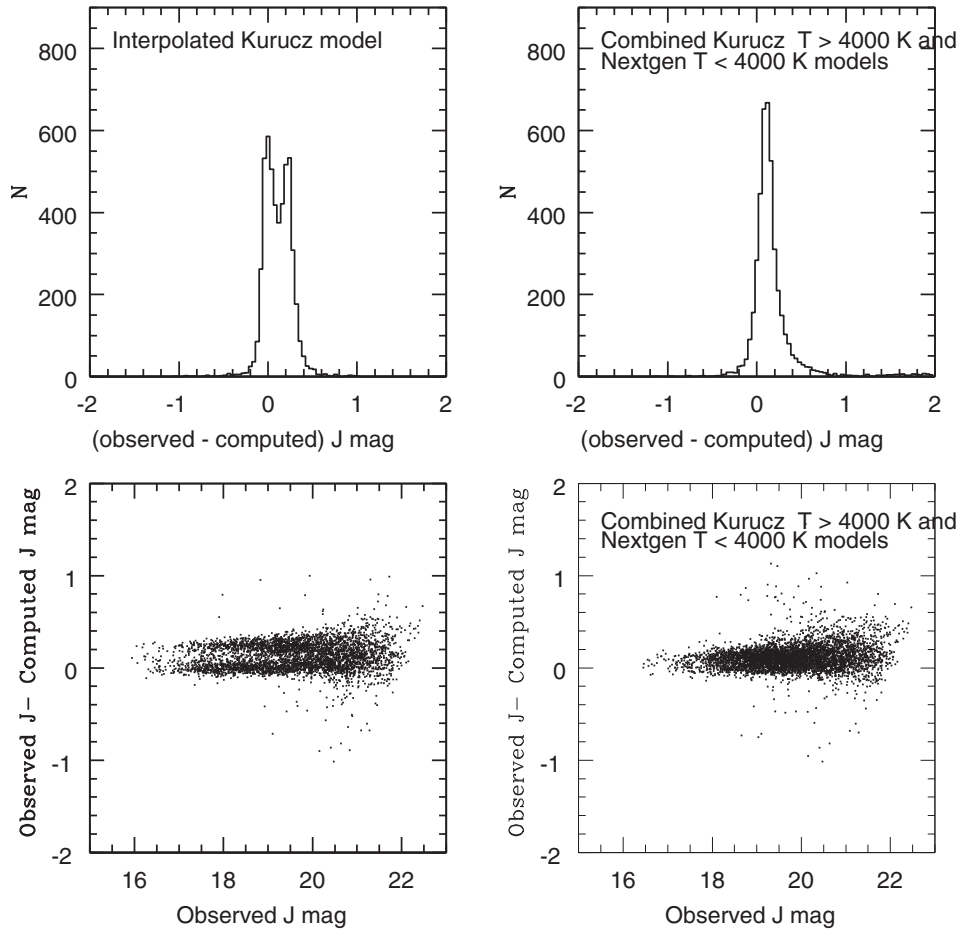


**Figure 20.** The difference between the observed and computed magnitudes are plotted against observed magnitudes for the sources in the test field, T2 are shown in lower panels (when combined model is used). The upper panels show the distribution of the difference between the observed and the computed magnitudes.

The combined model is interpolated with metallicity and gravity grid spacings are made finer to 0.25 dex with temperature grid spacings as it were. This model was also applied to the test field, T2 and the number of retrieved sources became 7077, which is 10% more than the previous combined model (which was not interpolated in gravity and metallicity) and the results were similar to that seen in the previous case. Thus the interpolated combined model is found to be the optimal model for the retrieval of maximum optically identified sources and hence the computation of their NIR magnitudes. The results from the combined model are given in Table 4.

## 6. Optimal method

We found that the optimal model for the retrieval of maximum number of optically identified sources and hence computation of their NIR magnitudes is the interpolated

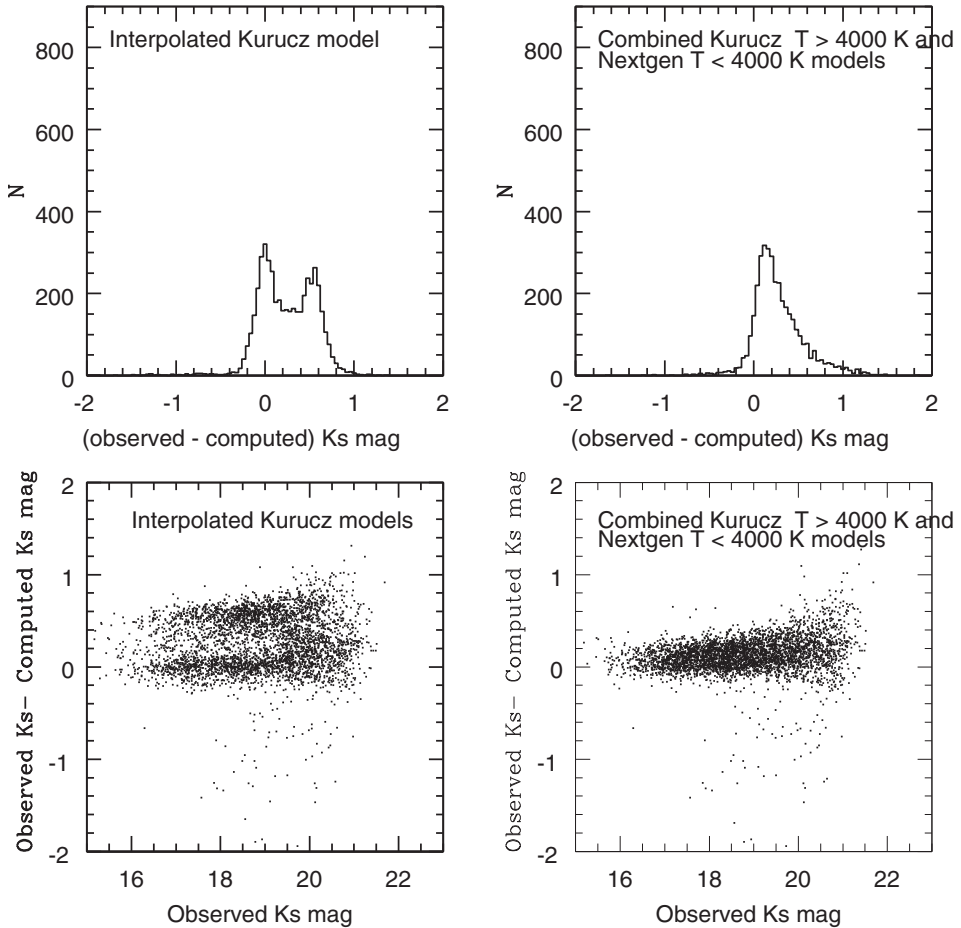


**Figure 21.** The difference between the observed and computed magnitudes are plotted against observed magnitudes for the sources in the test field, T2 are shown in lower panels (when combined model is used). The upper panels show the distribution of the difference between the observed and the computed magnitudes.

combined model of Kurucz ( $T > 4000$  K) and NextGen ( $3000 \text{ K} < T < 4000$  K) stellar atmospheric models. But at the same time, we can see from the upper right panels of Figures 20 and 21 that the single peak is slightly shifted towards positive values, indicating that the computed magnitudes are brighter by  $\sim 0.1$  mag and  $0.12$  mag than the observed ones in J and Ks bands respectively. When a combined model is used, for many of the sources an appropriate model is obtained from the NextGen model and we already saw from Table 3 that the computed magnitudes using NextGen models are relatively brighter than the observed ones, especially in the fainter magnitudes. Majority of these sources have parameters in the range  $3500\text{--}4000$  K and  $\log(g) > 3$ . From section 4.2, we can see that in this parameter range the Kurucz model reproduces the observed NIR magnitudes with required accuracy. The difference between the observed and the computed sources is also minimal with respect to zero difference. Thus in the combined model we need to include Kurucz

model instead of NextGen model in this parameter range also. For the parameter range,  $3000 \text{ K} < T < 3500 \text{ K}$  with all  $\log(g)$  values and  $3500 < T < 4000$  with  $\log(g) < 3$  we still need to use NextGen model. But as we saw earlier in Table 3, the computed magnitudes from NextGen model are relatively brighter than the observed magnitudes, especially in the cooler temperature regime. All these suggest that that we need to find an appropriate model for the sources in the optical catalog in two steps. First we need to use only the interpolated Kurucz model (with  $T > 4000 \text{ K}$  and also we can use the Kurucz models with parameters  $3500 \text{ K} < T < 4000 \text{ K}$  with  $\log(g) > 3$ ). Then the non retrieved sources are matched with the interpolated NextGen models with  $3000 \text{ K} < T < 4000 \text{ K}$ . Then the sources retrieved from this model are merged with those we obtained in the previous step. This we have illustrated for the test field, T2 and the results are shown below and in Fig. 22. In Fig. 22, the black histogram represents the results when interpolated Kurucz model was used for the computation of J magnitude. The red histogram represents the results when combined model (Kurucz models:  $T > 4000 \text{ K}$  and  $3500 \text{ K} < T < 4000 \text{ K}$  with

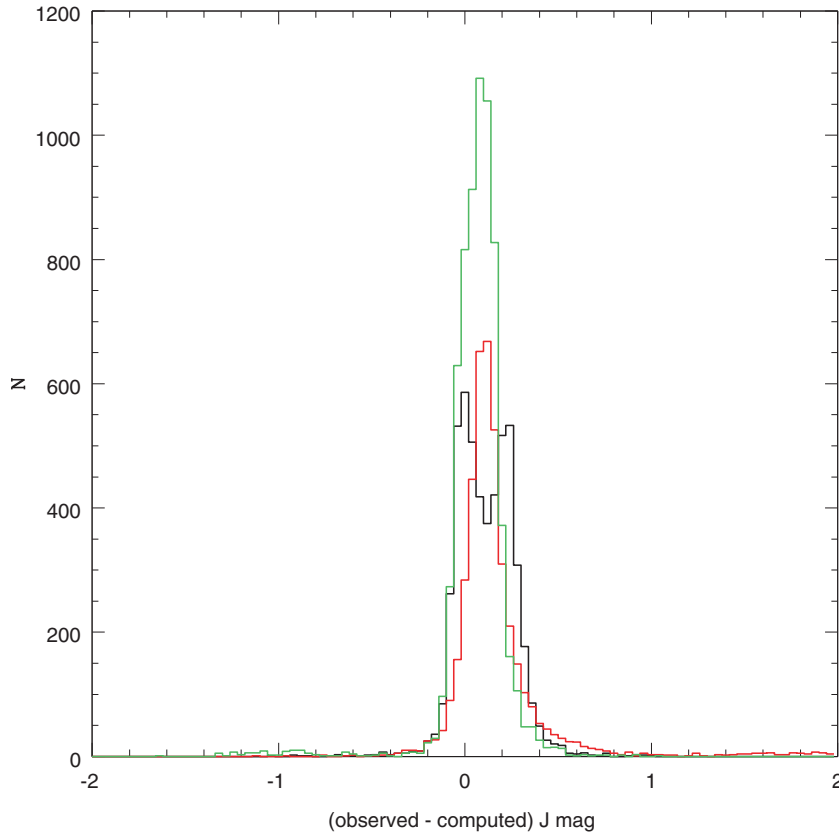


**Figure 22.** The black histogram represents the results when interpolated Kurucz model is used for the computation of  $J_{\text{Vega}}$  magnitude. The red histogram represents the results when combined model (Kurucz models:  $T > 4000 \text{ K}$  and  $3500 \text{ K} < T < 4000 \text{ K}$  with  $\log(g) > 3$ , NextGen models:  $T < 3500 \text{ K}$  and  $3500 \text{ K} < T < 4000 \text{ K}$  with  $\log(g) < 3$ ) is used. The green histogram represents the results obtained when combined model is used in two steps.

$\log(g) > 3$ , NextGen models:  $T < 3500$  K and  $3500 < T < 4000$  with  $\log(g) < 3$  is used. The green histogram represents the results obtained when combined model is used in two steps as described above. Figure 21 clearly shows that using combined model in two steps is the appropriate way to find an optimal stellar atmospheric model for the sources and hence the computation of NIR magnitudes (with a peak at  $\sim 0.08$  mag). The peak is dominated by fainter sources which are cooler sources and have their NIR magnitude estimates from NextGen model. An average shift of  $\sim 0.08$  mag is expected for sources with computed magnitudes obtained from Nextgen models.

Total number of sources in the optical catalog which are classified as stellar sources using the half-light radius criteria, for the test field T2 = 9298. The number of sources retrieved using the interpolated Kurucz model (Model 3) with temperature  $>4000$  K and also with temperature range 3500–4000 K with  $\log(g) > 3 = 3790$  (this number is just sufficient to satisfy the source density criteria of NFIRAOS). So, in principle, the next steps are not needed for this test field. But it is always better to have more number of sources and also in other fields this may not be the case. So we proceed to the next step.

Non retrieved sources = 5508

Number of sources retrieved when the interpolated NextGen models ( $3000 \text{ K} < T < 4000 \text{ K}$ ) are used = 3320

The total number of sources retrieved from the optical catalog (sources retrieved when Kurucz models + when NextGen models are used) = 7110

As the magnitudes computed using Kurucz models are very similar to the observed ones with minimal difference, the sources retrieved from the use of interpolated Kurucz models are the most reliable sources for using as guide stars. But if this number is not sufficient to satisfy the source density criteria of NFIRAOS, then we need to use the sources retrieved using the NextGen models. So in the merged catalog, we need to flag the ones obtained from the Kurucz model and from the NextGen models. The estimates from NextGen models can be used but they may have an average shift of  $\sim 0.08$  mag from the actual observed magnitudes. Thus preference should be given to the sources retrieved using the Kurucz models. The limitation of the developed methodology is mainly the non availability of accurate stellar models in the cooler temperature region.

## 7. Stellar models for star/galaxy classification

For the generation of IRGSC, an optimal star/galaxy separation is required. The application of stellar atmospheric models for the optimal star/galaxy classification is checked in two test fields, from the HST archival data (in three optical bands). The stellar and non-stellar sources in the catalog flagged with high probability (based on SExtractor flags) are taken for the analysis. The Kurucz stellar atmospheric model for the HST filters are interpolated and the synthetic colours are matched with observed colours. When the flags of the recovered and non-recovered sources are checked we found that almost equal fraction of stellar and non-stellar sources are there in both groups. As we are limited with data in only three wavelength bands, the stellar

atmospheric models alone cannot be applied for star/galaxy classification. An initial classification based on half-light radius/colour–colour diagram is needed and then the application of stellar atmospheric models, will help to do star/galaxy classification to a certain extent. The image quality of CFHTLS data is  $\sim 0.8$  arcsec in *g/r* bands and  $\sim 0.6$  arcsec in *i/z* bands. An image with similar or better image quality is one of the basic requirements of the optical catalog to be used for the final production of IRGSC.

## 8. Steps for the generation of GSC

The steps involved in the generation of GSC from optical data are as follows:

- (1) Identify the stellar sources with the extended star/galaxy classification. These are the probable stellar sources for which we need to compute the NIR magnitudes.
- (2) The interpolated Kurucz model ( $T > 4000$  K and  $3500 < T < 4000$  K with  $\log(g) > 3$ ) are used initially to identify the appropriate model for the sources and hence to compute the NIR magnitudes.
- (3) The sources which are not retrieved from the optical catalog after the second step are matched with the interpolated NextGen model ( $T < 3500$  K and  $3500 < T < 4000$  K with  $\log(g) < 3$ ) to identify the appropriate model for the remaining sources in the optical catalog and compute the NIR magnitudes.
- (4) The sources retrieved from Step 2 and Step 3 are merged to form the final catalog and the sources which are retrieved using Kurucz and NextGen models have to be flagged separately. The code for all the four steps is verified during its application for the test fields which are described in previous sections. The code is written to compute NIR magnitudes in the UKIDSS filters. We can change the filters based on our requirements. The errors associated with the computed magnitudes can also be estimated.

### 8.1 GSC from CFHTLS data

The test fields used in the present study are taken from CFHTLS fields. The CFHTLS fields are high latitude fields. The modified methodology based on stellar atmospheric models can be adopted to create a GSC for the whole CFHTLS data. As the methodology is verified using the observed NIR data, we can straight away run the code developed for the identification of the appropriate model for the stellar sources in the optical catalog and hence the computation of the NIR magnitudes. The CFHTLS optical data is deep enough for the generation of NIR magnitudes with limiting magnitude  $J_{\text{Vega}}$  up to 22 mag. We need stellar sources with magnitude up to  $I_{\text{AB}} \sim 23$  mag to obtain a NIR catalog of sources with  $J_{\text{Vega}}$  up to 22 mag. The CFHTLS does not cover the entire TMT observable sky. Hence the CFHTLS data cannot be used for the final production of the TMT IRGSC.

### 8.2 Analysis of Pan-STARRS data

Panoramic Survey Telescope and Rapid Response System (Pan-STARRS) is a survey of objects on a continual basis in the visible sky of Hawaii. It is expected to provide accurate astrometry and photometry of all the detected objects. The first

Pan-STARRS telescope, PS1 is located at Hawaii, went online in 2008. PS1 began full-time science observations in 2010 and the PS1 Science Mission is underway. The photometric observations are in  $g$ ,  $r$ ,  $i$ ,  $z$  and  $y$  filters. The limiting magnitude of Pan-STARRS is  $\sim 24$  mag in the  $r$  band. All the above mentioned properties of the Pan-STARRS make it one of the potential source for the production of the final TMT IRGSC. The reference data from Pan-STARRS is publicly available. The data provides reference PS1 photometry for 1-degree wide bands across the sky. There are 24 rungs in RA (1 at each integer RA hour) and 4 rungs in DEC (at  $-25$ ,  $0$ ,  $+25$  and  $+50$  degrees) which basically covers the entire latitude range we would like to have. In each band, a maximum of  $\sim 1000$  objects per square degree are provided. As this data do not include faint population, this is not sufficient to check whether the Pan-STARRS data can be used to produce the IR catalog with  $J_{\text{Vega}}$  up to 22 mag and also to check the number density criteria of NFIRAOS. But the analysis of this data is helpful to get familiarized with one of the future potential data sets for the generation of IR catalog. The catalog paper, (Magnier *et al.* 2013), provides a method to define stellar locus in the colour-colour diagram and this helps to extract the stellar sources in the catalog. We took a sample 1 square degree field and applied the criteria

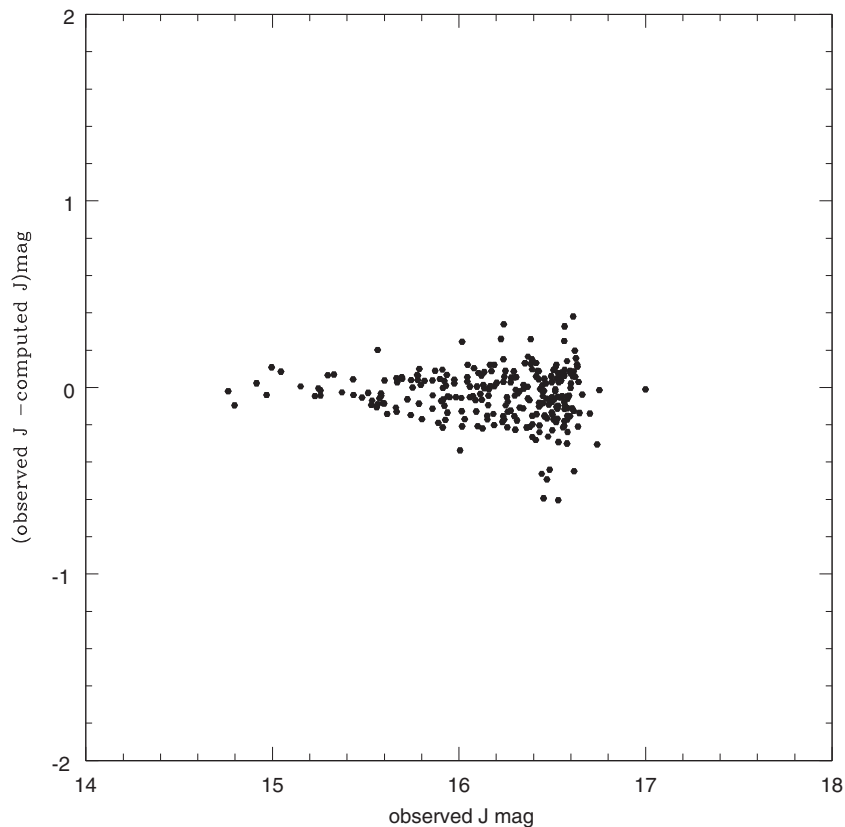


**Figure 23.** For the probable stellar sources from the Pan-STARRS reference catalog, the difference between the observed and computed J band magnitudes are plotted against the observed J band magnitude.

to extract the stellar sources. In the catalog paper they have defined a spline function to extract the stellar sources, but as an initial step we did a linear fit to extract the stellar sources from the  $(g - r)$  vs  $(r - i)$  colour-colour diagram. We applied the modified methodology, incorporating the interpolated stellar atmospheric models, to compute the IR magnitudes of the extracted stellar sources. The PS1 reference catalog also provides the 2MASS JHKs magnitudes of sources which are available. We compared the computed magnitudes with the observed 2MASS JHKs magnitudes. The results are illustrated in Fig. 23. This comparison is for a magnitude range of 14.5–17 mag in the J band. The computed and the observed magnitudes match within 0.2 mag, with a larger spread in the fainter magnitudes. Thus the analysis gives a promising result regarding the prediction capability of Pan-STARRS for the production of IRGSC for TMT observations. But a detailed analysis using a deeper data is required to check the magnitude limit and source density criteria (after the release of PS1 optical catalog). The final catalog of Pan-STARRS data is expected to have the required positional and photometric accuracies for the TMT IRGSC (private communication with the Pan-STARRS consortium, need to get a proper reference) and hence makes it a potential source for the production of the final IRGSC for TMT observations.

### 9. Effect of variable/high extinction in the NIR magnitude of guide stars

The extinction of the region plays an important role in the computation of the NIR magnitudes from their optical magnitudes and hence in the production of the final guide star catalog. The methodology developed here incorporates the effect of extinction. For each test field, the reddening value is taken from Schlegel *et al.* (1998) and that value is applied to all the sources in one square degree field. As all these three test fields are above the galactic plane (see Table 1), the effect of reddening may be minimal. But for the production of final catalog the effect of reddening has to be accounted properly, especially in the galactic plane regions where effect of reddening can be high as well as variable within small scales. The effect of differential reddening in the computed NIR magnitudes needs to be addressed by studying and applying this method in the galactic plane regions. This is planned in our future study. In some of the regions with high extinction, like the galactic bulge, we may not even get enough stars in the optical bands to compute their NIR magnitudes. But these regions are important science targets for TMT, especially for IRIS. So to obtain guide stars in these fields, we may have to plan deep NIR observations of these regions.

### 10. Summary

*Modification of the methodology to compute the NIR magnitudes from their optical magnitude:* The methodology developed by S12 is modified using the combined model of interpolated Kurucz models ( $T > 4000$  K and  $3500 < T < 4000$  K with  $\log(g) > 3$ ) and interpolated NextGen models ( $3000 < T < 3500$  K and  $3500 < T < 4000$  K with  $\log(g) < 3$ ). The optimal method based on two steps to identify the appropriate model for the stellar sources in the optical catalog is found. The modified methodology is tested and validated for a magnitude range of  $J_{\text{Vega}} = 16\text{--}22$  mag, by comparing the computed magnitudes with the observed NIR magnitudes

obtained from UKIDSS surveys. The reduction of sources which show large deviation (difference between the computed and the observed magnitudes larger than 3 times the error) in the methodology based on stellar atmospheric models compared to the black body model, suggests that the modified methodology is effective in removing the non-stellar sources.

*Star/galaxy classification:* HST archival data (in three filters) in two test fields where the star/galaxy classification is done with high probability are analysed. It was found that the stellar atmospheric models alone with three bands magnitude information cannot classify the stars and galaxies optimally. A prior information on the star/galaxy classification based on the half-light radius and/or colour–colour diagram are needed for the optimal classification. Pan-STARRS data have magnitude information in four bands ( $g, r, i, z$ ). This extra information in one band may help to improve the star/galaxy classification during the final production of IRGSC.

*Steps for the generation of GSC using CFHTLS data:* The steps to create a GSC using the CFHTLS optical catalog are identified based on the analysis of the test fields. The codes for the respective steps are written and tested. During the final production of the TMT IRGSC, we need to modify the codes for the respective optical filters.

*Analysis of initial Pan-STARRS data:* We analysed the public reference data of Pan-STARRS. The data is not deep enough to check the source density criteria, but it was used to get familiarized with the data. The modified methodology to compute the NIR magnitudes is applied to the sources (which are classified as stars based on the colour–colour diagram). The sources which have 2 MASS counterparts are identified and the observed and computed magnitudes are compared. The magnitudes are comparable and these results are promising for the future production of the IRGSC from Pan-STARRS data.

*Assessing the astrometric accuracies of Pan-STARRS data:* The information about the astrometric accuracies of the final Pan-STARRS catalog is obtained and the values satisfy the requirements of the IRGSC.

## References

- Castelli, F., Gratton, R. G., Kurucz, R. L. 1997, *A&A*, **318**, 841.  
 Girardi, L., Grebel, E. K., Odenkirchen, M., Chiosi, C. 2004, *A&A*, **422**, 205.  
 Gwyn, Stephen, D. J. 2008, *PASP*, **120**, 212.  
 Hauschildt, P. H., Allard, F., Baron, E. 1999a, *ApJ*, **512**, 377.  
 Hauschildt, P. H., Allard, F., Ferguson, J., Baron, E., Alexander, D. R. 1999b, *ApJ*, **525**, 871.  
 Kurucz, R. L. 1992a, *Rev. Mexicana Astron. Astrofis.*, **23**, 45.  
 Kurucz, R. L. 1992b, in: IAU Symp. 149, *The Stellar Populations of Galaxies*, edited by B. Barbuy and A. Renzini (Dordrecht: Kluwer), 225.  
 Kurucz, R. L. 1993, *ASPC*, **44**, 87.  
 Kurucz, R. L. 1995, Kurucz CD-ROM 13, *ATLAS9 Stellar Atmosphere Programs and 2 km/s Grid* (Cambridge: SAO), revised.  
 Magnier, E. A., Schlafly, E., Finkbeiner, D. *et al.* 2013, *ApJS*, **205**, 20.  
 Schlegel, David J., Finkbeiner, Douglas P., Davis, M. 1998, *AJ*, **500**, 525.  
 Subramanin, S., Subramaniam, A., Simard, L. *et al.* 2013, *JApA*, **34**, 175.